25/11/12/96 JSD

Bechtel Nevada

THE
REMOTE
SENSING
LABORATORY
OPERATED FOR THE U.S.
DEPARTMENT OF ENERGY BY BECHTEL NEVADA

DOE/NV/11718-013
UC-702
APRIL 1996

IN SITU RADIOLOGICAL SURVEYING AT THE DOUBLE TRACKS SITE

NELLIS AIR FORCE RANGE
TONOPAH, NEVADA

DATES OF SURVEYS: APRIL 10-13, 1995, AND JUNE 5-9, 1995

DISCLAIMER

This report has been reproduced directly from the best available copy.

Available to DOE and DOE contractors from the Office of Scientific and Technical Information, P.O. Box 62, Oak Ridge, Tennessee 37831; prices available from (615) 576-8401.

Available to the public from the National Technical Information Service, U.S. Department of Commerce, 5285 Port Royal, Springfield, Virginia 22161.

Bechtel Nevada

DOE/NV/11718-013
APRIL 1996

IN SITU RADIOLOGICAL SURVEYING AT THE DOUBLE TRACKS SITE

NELLIS AIR FORCE RANGE
TONOPAH, NEVADA

DATE OF SURVEY: APRIL 10-13, 1995, AND JUNE 5-9, 1995

S. R. Riedhauser
W. J. Tipton
Project Scientists

REVIEWED BY

Harvey W. Clark Jr.
H. W. Clark, Jr., Manager
Radiation Science

This Document is UNCLASSIFIED

Thomas M. Hayes
T. M. Hayes
Authorized Derivative Classifier

This work was performed for the United States Department of Energy by Bechtel Nevada under Contract Number DE-AC08-96NV11718 and by EG&G/EM under Contract Number DE-AC08-93NV11265.

ABSTRACT

A team from the Remote Sensing Laboratory conducted a series of *in situ* radiological measurements at the Double Tracks site on the Nellis Air Force Range just east of Goldfield, Nevada, during the periods of April 10-13 and June 5-9, 1995. The survey team measured the terrestrial gamma radiation at the site to determine the levels of natural and man-made radiation. This site includes the areas covered by previous surveys conducted from 1962 through 1993.

The main purpose of the first expedition was to assess several new techniques for characterizing sites with dispersed plutonium. The two purposes of the second expedition were to characterize the distribution of transuranic contamination (primarily plutonium) at the site by measuring the gamma rays from americium-241 and to assess the performance of the two new detector platforms. Both of the new platforms performed well, and the characterization of the americium-241 activity at the site was completed.

Several plots compare these ground-based system measurements and the 1993 aerial data. The agreement is good considering the systems are characterized and calibrated through independent means.

During the April expedition, several methods for measuring the depth distribution of americium-241 in the field were conducted as a way of quickly and reliably obtaining depth profiles without the need to wait for laboratory analysis. Two of the methods were not very effective, but the results of the third method appear very promising.

CONTENTS

Figures

Tables

Appendix

1.0 INTRODUCTION

The U.S. Department of Energy (DOE) maintains the Remote Sensing Laboratory (RSL), which provides several systems for measuring terrestrial radiation. In addition to the aerial radiological surveillance systems mounted in either BO-105 helicopters or B-200 airplanes, RSL has several systems for ground-based measurements. During these expeditions, RSL was operated by EG&G Energy Measurements, Inc., (EG&G/EM) under contract to DOE, with bases of operation at Nellis Air Force Base in Las Vegas, Nevada, and at Andrews Air Force Base near Washington, D.C.

The Double Tracks site was previously surveyed by the RSL from helicopter platforms in 1977 and 1993. The DOE requested that International Technology Corporation (IT) characterize the nature and extent of contamination, so that corrective action options could be evaluated. If necessary, the site would be cleaned up prior to its release back to the U.S. Air Force. Teams from the RSL participated in two ground-based expeditions to the Double Tracks site in the first half of 1995.

The first RSL expedition was performed from April 10-13, 1995, using the RSL's Chevrolet Suburban vehicle with a high-purity germanium (HPGe) detector mounted on its 7.5-m (25-ft) mast and two tripod HPGe detector systems. The objectives of this survey were to gather *in situ* radiological data with a set of different instruments at a series of locations within the Double Tracks exclusion zone (fenced area) and to compare this data with similar data collected by previous aerial surveys and by systems fielded by IT and Reynolds Electrical and Engineering Co, Inc. (REECo).

Based on the information acquired during the first trip, a second expedition took place during the week of June 5-9, 1995, when two new detector platforms were field tested. One platform used a set of three Field Instrument for Detection of Low-Energy Radiation (FIDLER) detectors mounted on the front of an all-terrain vehicle (ATV) about one-half meter above the ground. This system was used to search in a systematic manner for pieces of metal which had plutonium (Pu) adhering to their surfaces. The second detector platform fielded during this trip was the standard RSL aerial detection and recording system adapted to a ground-based vehicle and nicknamed the Kiwi. Specifically, a set of sodium iodide (NaI) detectors were mounted on the rear of a Chevrolet Suburban vehicle. As the vehicle moved, individual gamma-ray spectra were recorded each second to provide complete coverage of the Double Tracks area. The field-of-view of the detector system was approximately 3 m (10 ft) in diameter.

For consistency between this report and the *Double Tracks Test Site Characterization Report* being prepared by IT, the phrase "hot fragment" will refer to any piece of radioactive material larger than 5 μm (0.0002 in). Pieces smaller than this size will be called "hot particles." The term "piece" will refer to either a fragment or a particle. Any piece which is visible to the unaided eye is a fragment.

2.0 SURVEY SITE DESCRIPTION

The Double Tracks site is situated on Stonewall Flat (an arid plain) on the Nellis Air Force Range (NAFR) and is about 25 km (16 mi) east of Goldfield and 35 km (22 mi) southeast of Tonopah, Nevada.[1] Access is through the Tonopah Test Range (TTR). The Double Tracks site has an elevation of approximately 1,500 m (4,900 ft). The area is mostly sandy soil with a thin layer of small gravel on the surface and is covered with small shrubs and some grass. The Double Tracks test involved the detonation of a high explosive near an assembly of Pu and depleted uranium (U) to study the means of dispersal of transuranic (TRU) elements and their uptake in animals. The quantity of depleted U was 4-5 times the quantity of Pu. The test was conducted at 2:55 a.m. on May 15, 1963.

The five-sided fence currently surrounding the Double Tracks site forms the radiation exclusion zone of approximately 18 hectares (2 million ft^2). This fence was established several years after the test and the boundary was based on the gamma radiation levels measured by a set of FIDLER detectors. After the test, soil from an area near the blast was pushed on top of the original concrete platform to produce a mound about 1.3 m (4 ft) high. An older, almost circular fence still existed (until the June expedition) around the mound of soil at ground zero (GZ) and extended 30-40 m (100-130 ft) from GZ.

Previous semiannual ground-based surveys of the Double Tracks site were conducted by REECo for several years after the tests.[2] These surveys consisted of air samples, surface swipes, and water examination, as well as gas proportional counter measurements made in the four compass directions at 30-m (100-ft) intervals from the (what is now inner) fence. As described in the REECo report, these measurements were strongly influenced by high-activity debris near the measurement locations.

RSL performed aerial surveys of the Double Tracks site using helicopters in February 1977 and December 1993. The 1977 survey was conducted at a 30-m (100-ft) altitude using a line spacing of 61 m (200 ft).[3] The 1993 survey was also conducted at a height of 30 m but used a line spacing of 46 m (150 ft).[4] A separate report presents additional processing of the 1993 data to improve the minimum detectable activity for americium-241 (^{241}Am).[5] However, this additional processing had the deleterious side effect of enlarging the footprint of the measurement system and decreasing the spatial resolution of the data thus distorting the size of the area which needed remediation.

3.0 NATURAL BACKGROUND RADIATION

Many factors—both radiation from sources of interest to the current investigation, radiation from sources not of current interest, and electrical noise—contribute to forming the total measured gamma-ray energy spectrum. These components can be summarized as the five terms in the following equation:

$$\left[\begin{array}{l}\text{Measured}\\ \text{Radiation}\\ \text{Spectrum}\end{array}\right] = \begin{array}{l}\text{Natural Terrestrial Radionuclides}\\ +\ \text{Man-Made Radionuclides}\\ +\ \text{Airborne Radon}\\ +\ \text{Cosmic Rays}\\ +\ \text{Equipment Contributions}\end{array} \qquad (1)$$

The term "natural background radiation" is generally considered to comprise three of the terms in the above equation; namely, natural terrestrial radionuclides, airborne radon (Rn) gas and its daughter products, and cosmic rays. The man-made radionuclides, such as cobalt-60 (^{60}Co) and cesium-137 (^{137}Cs), produced through actions by man are generally the components of the radiation field of most interest. The final term in this equation represents all sources of "noise" in the final spectrum, ranging from electrical noise in the electronics processing the detector signals to radiation sources inherent in the detectors and other measurement equipment.

Long-lived radionuclides present in the earth's crust are usually the largest source of background radiation. Naturally occurring isotopes found in the soil and bedrock consist mainly of radionuclides from the U and thorium (Th) decay chains and radioactive potassium (K). The most prominent natural isotopes usually seen in spectra are potassium-40 (^{40}K) (0.012% of natural K), thallium-208 (^{208}Tl) and actinium-228 (^{228}Ac) (daughters in the ^{232}Th chain), and bismuth-214 (^{214}Bi) (a daughter in the ^{238}U chain). Although it is considered a man-made radionuclide, a measurable amount of ^{137}Cs is found throughout the world (initially as a surface deposition and then, over time, migrating several inches into the soil) as a result of the atmospheric testing of nuclear weapons. These naturally occurring isotopes typically contribute 1-15 μR/h to the background radiation field.[6]

Rn (a noble gas) is a member of both the U and Th decay chains. After being created in the soil from its parent isotope, Rn can diffuse through the soil and become airborne. While the isotopes of Rn have relatively short half-lives, their daughters may become attached to dust particles in the atmosphere and contribute to the airborne radiation field until the dust eventually settles to the ground. The contribution of Rn and its daughters to the background radiation field depends on several factors, including the concentration of U and Th isotopes in the soil, the permeability of the soil, and the meteorological conditions at the time of measurement. Typically, airborne radiation from Rn and its daughters contributes 1-10% of the natural background radiation level.

Cosmic rays entering the earth's atmosphere are a third source of background radiation. High-energy cosmic rays (principally protons, alpha particles, and some heavier nuclei) interact predominantly with atoms in the upper atmosphere to produce showers of secondary radiation. The contribution of cosmic rays to the background radiation field varies with elevation above mean sea level and with geomagnetic latitude. The earth's magnetic field traps some of the cosmic rays, so a larger fraction of them reaches the poles than the equator. In the continental U.S., values range from 3.3 μR/h at sea level to 12 μR/h at an elevation of 3,000 m (10,000 ft).[7] For surveys in the continental U.S., the dependence on geomagnetic latitude is very small and the elevation of the survey is the predominant determinant of the cosmic ray flux.

4.0 SURVEY EQUIPMENT AND PROCEDURES

Each radioactive isotope emits one or more types of radiation when it decays—alpha particles, beta particles, gamma rays, or X-rays. More importantly, these decay products have a specific energy which helps to indicate what parent isotope emitted it. The mix of Pu isotopes present at Double Tracks decay either by the emission of an alpha particle (which is

impossible to detect more than a few centimeters away) or by the emission of a very low-energy beta particle (which is also very difficult to detect). In addition to these particles, Pu emits some low-energy X-rays and, at a very low rate, some gamma rays. Nearly all systems used to search for Pu rely on detecting the 60-keV gamma ray emitted by ^{241}Am, the decay product of plutonium-241 (^{241}Pu). These gamma rays are relatively easy to detect, even from aerial detection systems 30-50 m (100-150 ft) above the ground, and are much more abundant than the gamma rays emitted directly from the Pu decays.

The NaI detectors (used in the Kiwi system and by previous aerial surveys) can be made with large areas and volumes which allow them to efficiently collect most of the gamma rays incident on their crystal face. However, their energy resolution is relatively poor, so the ability to identify specific gamma-ray energies and, therefore, specific isotopes is limited to areas containing only a few isotopes. The HPGe detectors (used on the Suburban system and on the tripods) are much smaller in size than the NaI detectors. Consequently, they collect gamma rays at a much lower rate. Their advantage is their high-energy resolution, which makes the isotopic identification relatively easy even in areas containing many isotopes.

The above discussion regarding the identification of isotopes from the measured gamma-ray energies assumes that all of the initial gamma-ray energy is collected by the detector. This is not often the case. Many of the gamma rays emitted by an isotope will be scattered (by soil or air or inside the detector) and lose some of their energy, breaking the correlation between a specific energy and a specific isotope. This is a process known as Compton scattering, and it creates a smoothly varying background within the energy spectrum. Statistical fluctuations at a given energy due to this Compton background increase the uncertainty in how many gamma rays of this initial energy were detected. Thus the uncertainty in the amount of an isotope present during a measurement increases with the increase in the Compton background.

Unlike alpha and beta particles, gamma rays can travel large distances through the atmosphere. With a detector suspended 1 m (3 ft) above a perfectly flat ground, 50% of the detected 60-keV ^{241}Am gamma rays will originate from more than 6 m (20 ft) away. Typical ground-roughness effects will decrease the number of gamma rays from large distances, but a 6-m radius circle is still not a very localized area. When a measurement must be made of a well-defined spot on the ground, a collimator must be used to shield the detector from gamma rays emitted from areas outside this one spot. Generally, limiting the field-of-view requires the use of a large quantity of very dense material. However, for 60-keV gamma rays, this can be accomplished by using approximately 3mm (1/8 in) of lead (Pb).

The following paragraphs present a sketch of the data collection procedures used for this survey. Each of the experiments used a specific means of obtaining positioning information. The Kiwi used a differential global positioning system (GPS), licensed from John Chance Corporation, which has a positioning uncertainty of less than 1 m (3 ft). The HPGe Suburban has a slightly less accurate differential GPS system, which yields an uncertainty of 3-5 m (10-16 ft). Some of the locations measured by the Suburban in June were centered over locations marked by stakes in a circular grid which dates back to the 1960s. The 0° reference of this circular grid appeared to be aligned with magnetic north, rather than the polar north implicit in the latitude, longitude coordinates of the GPS. The difference between polar north and magnetic north is about 15° in the Double Tracks area. Most of the measurements made with the tripod detector systems and some of the Suburban measurements are referenced to this circular grid.

The coordinates listed in the literature for GZ are 37°42′22.52″ N and 116°59′14.23″ W in the NAD27 coordinate system.[3] The GPSs used when collecting the data in this report are referenced to the WGS84 coordinate system. For the Double Tracks area, the U.S. Geological Survey (USGS) guidelines instruct one to move the NAD27 grid by 10 m (33 ft) (0°0′0.32″) N and 79 m (259 ft) (0°0′3.23″) E to convert the position into the WGS84 system. Applying this to the GZ position quoted above yields a position of 37°42′22.20″ N and 116°59′17.46″ W in the WGS84 system.

While no GPS measurements were made at GZ, Suburban-system measurements were made at the 30-m (100-ft) positions on the circular grid at 0°, 90°, 180°, and 270°. These four measurements yield an average GZ position of 37°42′21.95″ N and 116°59′17.80″ W (in the WGS84 coordinate system). This average position is only 7.7 m (25.3 ft) (0°0′0.25″) S and 8.4 m (27.6 ft) (0°0′0.34″) W of the published location.

The April survey made a number of isolated measurements and did not cover the whole Double Tracks area. In June, the Kiwi covered all of the area inside the fence as well as a few test spots south of the

fence. The ATV covered most of the area inside the fence less than 152 m (500 ft) from GZ.

4.1 Experiment #1 (April)—HPGe *In Situ* Measurements

This experiment was designed to provide a correlation between the various methods of ground-based data taken during the April survey and, if possible, a comparison with the aerial data taken in December 1993. To this end, a series of measurements with the different instruments was taken in the same area. First, a four-wheel drive vehicle (Chevrolet Suburban, see Figure 1) with a collimated HPGe detector suspended on a mast 7.5 m (25 ft) above ground level (AGL) made a set of measurements across an area identified by the aerial data as having a relatively constant ^{241}Am concentration. The collimated detector views a circular area with a diameter of approximately 13 m (43 ft). In comparison, the aerial system made measurements with a 100-m (330-ft) diameter spatial resolution.

At several of these locations, the mast was lowered and an additional measurement was made with the detector only 3 m (10 ft) AGL. At this height, the field-of-view for the ^{241}Am 60-keV gamma rays is approximately 5.2 m (17 ft). In addition to these comparison measurements, a number of isolated Suburban and tripod measurements were made throughout the fenced area.

4.1.1 Suburban Versus Tripod Measurements

Following the measurements taken by the Suburban system, a different HPGe detector, mounted on a tripod and placed 1 m (3 ft) AGL, made a set of measurements covering the area measured by the Suburban detector at a 3-m (10-ft) height. The tripod systems were collimated with a Pb shield to produce a field-of-view for the low-energy ^{241}Am 60-keV gamma rays of approximately 2 m (6.6 ft). To minimize the number of measurements needed, the measurements were made using a triangular grid pattern. Thus the Suburban footprint could be almost covered by seven tripod measurements.

Following the tripod measurements, systems fielded by REECo and the Oak Ridge National Laboratory (ORNL) made their measurements in this same area.

4.1.2 Measurements South of the Exclusion Fence

A series of nine measurements was made south of the fenced area using a tripod-mounted HPGe detector. Measurements were made to corroborate the results obtained from the December 1993 aerial survey,

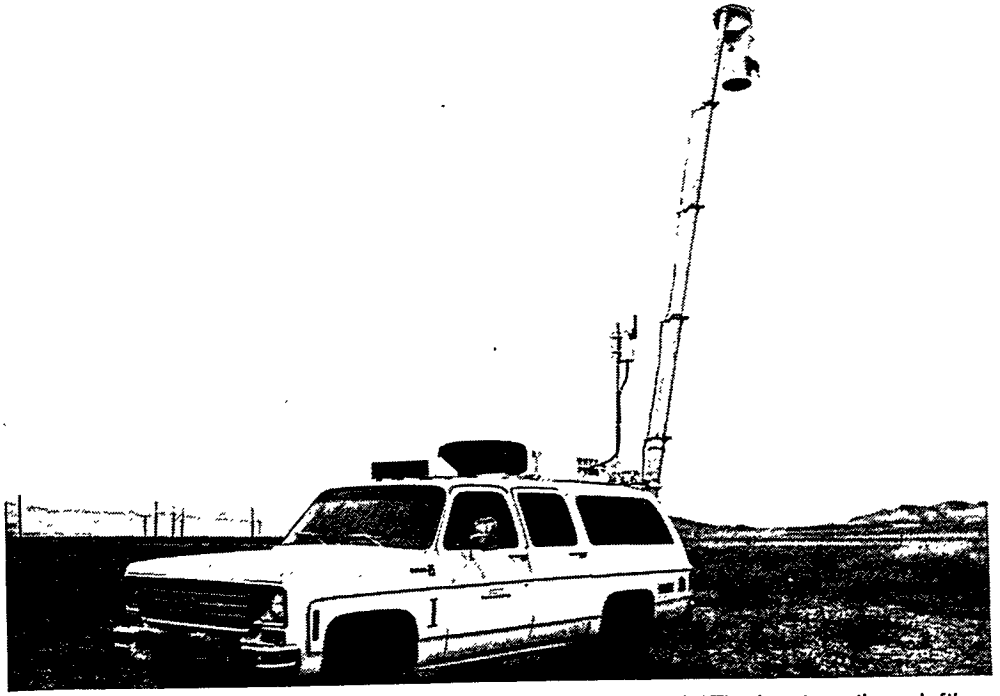

FIGURE 1. ***SUBURBAN VEHICLE WITH HPGE DETECTOR ON MAST.*** *The detector on the end of the mast can be extended up to 7.5 m above the ground.*

which indicated a very low-level plume extending from the southern fence. Since there were no means to determine an exact position with this system, an attempt was made to pace off distances along the concentration center line of the plume using a compass for reference. The actual measurement line, however, deviated somewhat from the planned line.

4.2 Experiment #2 (April)—Pu:Am Ratio Measurements

The experiments performed at Double Tracks in April were intended to determine the nature and extent of TRU contamination by detecting gamma rays. All of the measurements rely on detecting the 60-keV gamma rays emitted by ^{241}Am, a daughter of ^{241}Pu, and inferring the amount of Pu and TRUs through a combination of field measurements and theoretical considerations.

The activity levels in the eastern part of the central mound were high enough to allow direct measurement of the very weak gamma rays from ^{239}Pu at 129 keV, 375 keV, and 414 keV. The 129-keV gamma ray is approximately 6,000 times less intense per disintegration than the 60-keV gamma ray from Am. The other two Pu gamma rays are approximately 23,000 times less intense. The Pu:Am ratio is usually obtained in the laboratory using small soil samples that are chemically dissolved and then analyzed using alpha spectrometry. However, the physical characteristics of Pu make this laboratory analysis very difficult. Because the activities at the Double Tracks site are large enough, *in situ* measurements are capable of accurately measuring the gamma rays from Pu. Thus the TRU:Am ratio calculated from the *in situ* data will have a better accuracy than the ratio from the laboratory analysis.

Two independent methods of measuring of the Pu:Am ratio were performed. The actual location on the mound was approximately 12 m (40 ft) from GZ and about 105° E of magnetic north (referenced to the circular grid). The first method used an HPGe detector mounted on a tripod 1 m (3 ft) AGL. The first set of measurements using this system left the detector uncollimated and the gamma-ray spectrum was written to tape at the end of 10-, 20-, and 30-minute periods. The second set of measurements used a Pb collimator to reduce the field-of-view to about a 2-m (6-ft) radius. The plan in using the collimator was to collect the 60-keV gamma rays from ^{241}Am and the 39-keV and 51-keV X-rays from ^{239}Pu from the same area. The use of the collimator was not as successful as originally anticipated. The large Compton background generated by the ^{241}Am gamma rays made the extraction of the small quantity of 39- and 51-keV gamma rays very difficult.

The second method to measure the Pu:Am ratio used a highly collimated, tripod-mounted HPGe detector. Measurements were made for 300 and 600 seconds. The measured gamma-ray count rates were then converted into the appropriate radioactivity values. To make this conversion for an *in situ* measurement, it is necessary to know or make assumptions on the depth distribution of the contaminant. Results are presented for assumed exponential distributions with relaxation lengths of 3, 20, and 100 cm (1, 8, and 40 in). The mound was formed by scraping the contaminated surface around the detonation site after the explosion, and this most likely led to contamination being mixed throughout the mound. In this case, a deeper depth distribution would be more representative of the contamination than the shallow distribution usually encountered due to weathering of surface Pu into the soil.

4.3 Experiment #3 (April)—Depth Profiling Measurements

The purpose of these measurements was to develop an inexpensive, fast (hopefully field-calculable) method of measuring the ^{241}Am depth distribution over large areas of contamination. The depth distribution is required to convert HPGe *in situ* count-rate data into soil activity concentration results. It is also critical for obtaining a reasonable estimate of the amount of contaminated material that might have to be removed. Currently, the established method is to take soil samples from selected depths and analyze the samples in the laboratory. This method involves transportation of contaminated soil, time to prepare the samples, and the counting time in the laboratory. The final results are also sensitive to the depth interval used for each sample. Usually, samples are taken in 2.5-cm (1-in) layers. This rather coarse sampling does not provide representative data for the shallow distributions typically encountered with Pu contamination. In typical Pu contamination situations, samples taken in 1- or 2-cm layers are usually required. Hot pieces, routinely found around the safety shot tests, also introduce a serious problem in obtaining useful data.

Three techniques were evaluated during the April field survey for obtaining depth profile data. These include the following:

- Side wall measurements with TLD material
- Comparison between the X-rays from ^{239}Pu and the gamma ray from ^{241}Am
- Direct measurement with highly collimated HPGe detector as thin layers of soil were removed

4.3.1 Side Wall Measurements with Thermoluminescent Dosimetry Material

Thermoluminescent material, when used for thermoluminescent dosimetry (TLD), can be used to measure surface alpha contamination. The TLD material used for these measurements ($CaSO_4$:Tm) is gamma insensitive, with a beta sensitivity approximately 100 times less than the alpha sensitivity. The alpha sensitivity is quite high with about one Read-Out Count (ROC) per disintegration per minute (dpm) and a large dynamic range in which the sensitivity is linear. This allows their use in mapping areas containing low to very high levels of radioactivity. Measurements made previously with this material in Area 11 of the Nevada Test Site (see Appendix B) accurately portrayed the erratic surface distribution of the TRU isotopes around those safety shot sites. It was found that a good deal of the contamination is in discrete "hot spots" that can cause rapid variations in activity levels over distances of only a few centimeters. This is why typical soil sample counting can produce widely varying results even for samples taken adjacent to each other. Because the material proved so successful for the surface measurements, an attempt was made to try to obtain similar results for depth profiles.

The TLD material was affixed to sheets 30 cm (12 in) on each side. Readout can be controlled to 1-mm (0.04-in) intervals in both the x and y directions, providing excellent spatial resolution for the measurements. Thirty-minute measurements are sufficient to obtain background alpha activity levels. The material was then sent to a laboratory for analysis. If these measurements are performed routinely, a film reading station could be purchased for field use. The film is reusable after it has been analyzed and read.

Six TLD sheets were used, in pairs, at three measurement locations. One sheet was placed on the surface. The other sheet was inserted into the ground by digging a small trench, placing the sheet against the wall, and then backfilling the trench to hold the sheet in place for the required exposure time. This created a "surface" approximately 25-30 cm (10-12 in) deep and 30 cm (12 in) across. The TLD sheet was held against the side wall for approximately 30 minutes. All three measurements were made near the inner fence south of GZ.

4.3.2 Comparison Between the Pu X-Rays and the ^{241}Am Gamma Ray

A second technique evaluated during the April expedition tried to measure the difference in the number of 60-keV ^{241}Am gamma rays compared to the number of 17- to 23-keV X-rays emitted during the decay of ^{241}Am and the various Pu isotopes.

Pu contamination is usually measured using the 60-keV gamma ray from ^{241}Am. It can also be detected using the L X-rays from the Pu and Am decay in the 17- to 23-keV range. For contamination near the surface, the X-ray region is useful. Due to the rapid attenuation of these low-energy X-rays in soil, however, the 60-keV gamma ray is more useful for activity that has migrated into the soil. The mass attenuation coefficient for soil at 20 keV is approximately ten times greater than at 60 keV. The X-rays will be attenuated much faster with depth in soil than the 60-keV gamma ray. This difference in attenuation may be able to provide an indicator of the contamination distribution with depth. To make the measurements, it is necessary to ensure that all radiation reaching the detector travels through the same depth of soil. This can be done using a long collimator that only allows radiation from directly below the detector to be counted. The ratio of the 60-keV gamma ray to one or more of the X-rays would then provide an indicator of the depth of the contamination.

With an HPGe detector mounted on a low tripod, a collimator was built that extended from the detector to the ground to ensure only radiation from directly below the detector would be counted. The collimator was made of tin (Sn) with an inner liner of copper (Cu). Since the collimator (as well as the detector) will be bathed by the gamma rays from the natural radionuclides, a fraction of the atoms will be excited by the gamma rays and will emit their own particular-energy X-rays. Thus, since the collimator material is going to emit X-rays which will be detected, the goal is to find a collimator material which adds the fewest counts to the particular-energy range of interest. Sn is somewhat better than Pb for these applications. Pb has K X-rays in the 70-90 keV range which increases the background in the 60-keV window. Pb also has L X-rays which extend into the Pu and Am X-ray window. Sn has K X-rays just above the Pu-Am window and L X-rays below this window. The Cu liner stops the K X-rays

and puts all possible interference from the collimator below the Pu-Am X-ray window.

Six measurements were made just inside and outside the inner fence. Measurements were made at the three locations where the TLD material measurements were conducted and at three additional areas where spot FIDLER measurements showed elevated activity.

4.3.3 Direct HPGe Measurements

The third technique that was evaluated directly measured the ^{241}Am activity level as thin layers of soil were removed. A detector was collimated to limit the field-of-view to an area approximately 40 cm (16 in) in diameter. Soil was then removed in layers approximately 1-3 cm (0.4-1.2 in) thick, with measurements made after each layer was removed. Spraying the soil lightly and uniformly with a little water allowed a person with a metal dustpan to scoop up a thin layer of soil and minimize the creation of blowing dust. A little practice was required to avoid getting the ground too wet too deep and to scoop up only a thin layer of soil. The soil was removed over an area larger than the field-of-view of the collimated detector to ensure that only the newly exposed surface was measured.

This method is similar to obtaining profile samples in the field and returning them to a laboratory for analysis. The primary differences are the much larger sample size counted (approximately 1,600 cm^2 [248 in^2] verses 100 cm^2 [16 in^2] for a typical soil sample) and the convenience of not having to transport soil from the site.

4.4 Experiment #4 (June)—ATV Hot-Piece Search

FIDLER detectors have been used extensively in the past for locating regions contaminated with ^{241}Am (and Pu by inference). Although the system only reports the total count rate observed in the detector, medium- or high-energy gamma rays are very unlikely to have any interaction with the very thin detector crystal. This makes the detectors insensitive to much of the variation in the natural terrestrial radioactive isotopes or to fallout isotopes such as ^{137}Cs.

During the April expedition, a hand-held FIDLER found many locations where the radioactivity level was elevated and very localized. In most of these cases, small pieces of metal with Pu and Am adhering to the surface were found in the area. Two locations were "mined" by IT personnel. "Before" and "after" measurements of these locations produced encouraging results (see Section 6.1). During the week of the April expedition, it became very clear that there were many localized regions near GZ with elevated activities.

The ATV experiment was included in the June expedition to test our ability to systematically locate and remove the fragmented pieces. A set of three collimated FIDLER detectors mounted on the ATV is shown in Figure 2. This system traveled east and west inside the fenced area within several hundred feet of GZ to look for hot pieces. The collimators on the detectors limited the fields-of-view to about a 0.6-m (2-ft) diameter on the ground. There was sufficient overlap between the fields-of-view to ensure that complete coverage was obtained over an area about 1.5 m (5 ft) wide.

Because this was still an experimental vehicle, the driver had to steer the ATV by keeping the tire tracks from the previous pass a constant distance to the side. While the ATV occasionally had to be maneuvered around some of the larger bushes, the amount of ground possibly missed by the detectors was very small. If the detected activity exceeded a set level, an alarm sounded. A larger than expected amount of time was spent at Double Tracks determining the optimum trip levels for the alarms on the detectors. It was finally determined that 50% above background was a reasonable level which resulted in finding many hot pieces and produced very few false alarms. (False alarms were often produced if the ATV bounced excessively while going over a bush or the edge of a small wash.)

When the alarm on one or more detectors sounded, the driver would stop and back over the area to verify that it was not a false alarm and then place a colored flag in the ground. A group of "miners" would go to each of the flagged locations with a hand-held FIDLER and shovels to find the hot piece and remove it from the area. Fragments were usually located immediately using the hand-held FIDLER, but after a while, the miners sometimes could recognize fragments visually before using the FIDLER. After removing the fragment, the FIDLER would be used to survey the immediate area for any flakes which may be left behind from the original fragment. In a few instances, the radiation was spread over a small area and a few shovels of soil and hot particles were excavated. The hot fragments and soil containing hot particles were

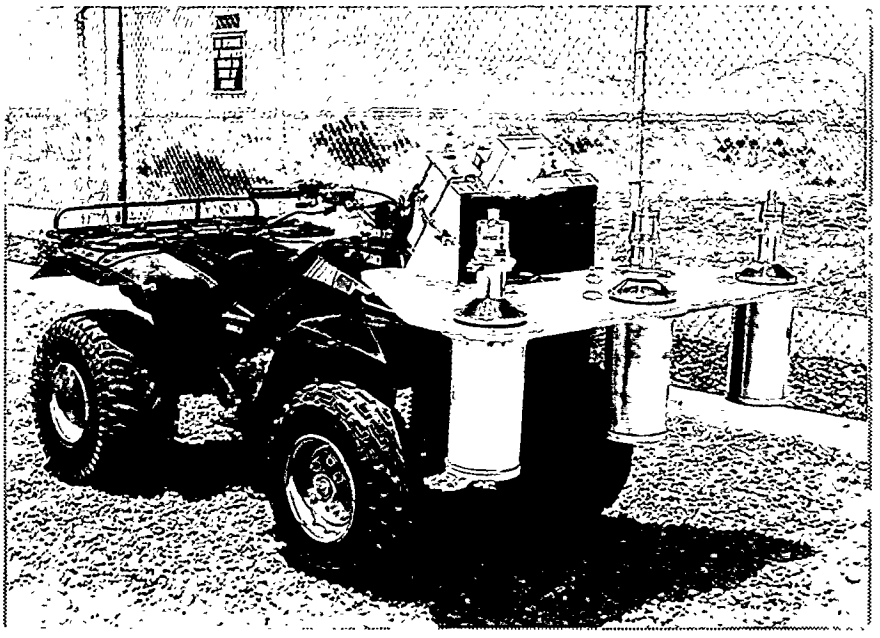

FIGURE 2. ***ATV WITH FIDLER DETECTORS.*** *The three detectors see slightly overlapping areas on the ground as the ATV travels at several feet per second. A sharp rise in the count rate by one of the detectors signifies a hot piece underneath that detector.*

placed in secured containers for later disposal during the clean-up operations.

4.5 Experiment #5 (June)—Kiwi Survey Measurements

The Kiwi system is the result of mounting the detectors and data collecting system from RSL's standard aerial system onto a Chevrolet Suburban vehicle (see Figure 3). Six 5- × 10- × 40-cm (2- × 4- × 16-in) NaI logs are housed in pods mounted on an angle-iron frame attached in place of the rear bumper. Signals from these detectors feed into a Radiation and Environmental Data Acquisition and Recorder (REDAR), Model IV, system bolted to the floor of the Suburban. Signals from the GPS constellation of satellites, received by the antenna mounted above the detectors, are preprocessed by a John Chance Corporation unit before feeding into the REDAR system. The second antenna, mounted on the roof of the Suburban, receives a correction signal from a network of GPS stations around the country. The signal is relayed through a dedicated satellite for John Chance Corporation subscribers. This correction signal reduces the uncertainty in positioning the vehicle to less than 1 m (3 ft) rather than the 3-5 m (10-15 ft) uncertainty in the earlier correction hardware employed in the helicopter system.

The Kiwi detectors are shielded on the back and sides with a sheet of cadmium (Cd) while the end-mounted photomultiplier tubes and the vehicle itself provide shielding to the front of the detectors. This shielding is more than adequate for attenuating the 60-keV gamma rays of ^{241}Am but does not significantly affect the higher energy radiation from the natural radioisotopes. The shielding produces a well-defined footprint for making assessments of the Am concentration in a given volume of soil. Thus the ^{241}Am footprint of the stationary Kiwi system is about 3 m (10 ft) in width and 1.2 m (4 ft) long. With the Kiwi traveling at 2.2 m/s (5 mph; 7 ft/s), the footprint is about 3 m (10 ft) wide by 3.4 m (11 ft) long.

Just like the aerial platforms, the REDAR system in the Kiwi was programmed with a set of "flight" lines to travel during the survey. For simplicity and to minimize the amount of time needed to turn around inside the fence, the lines were arranged parallel to the western fence making them almost due north-south. The GPS position was compared to this preferred flight path each second, and the deviation (left or right) from the line was displayed for the driver on a meter mounted above the dashboard. The flight lines were only 3 m (10 ft) apart. With the rough terrain in several spots, some deviation from the planned flight lines was necessary.

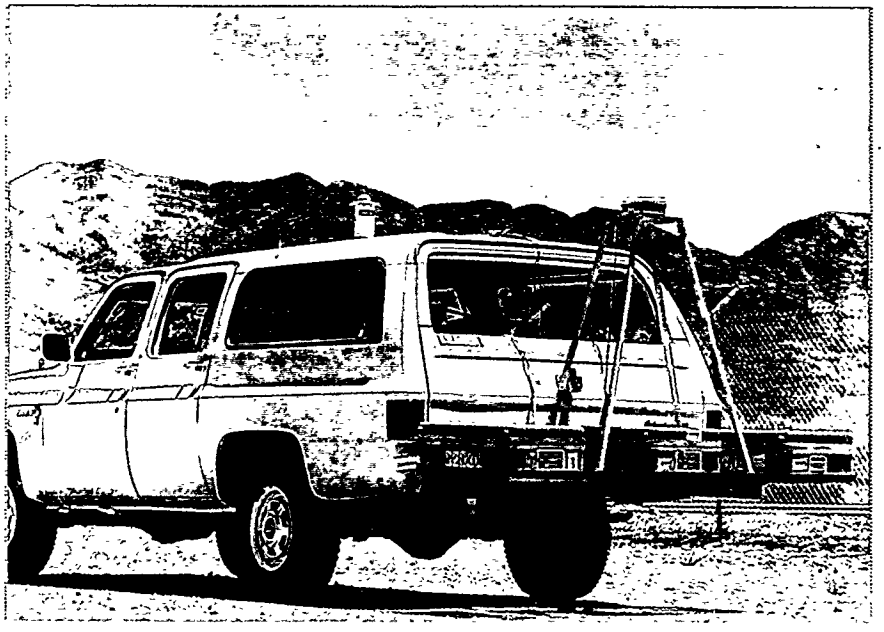

FIGURE 3. *KIWI VEHICLE. Six NaI logs in the three pods on the rear of the Suburban vehicle detect gamma rays from Am. Shielding on the sides of the detectors limits the field-of-view to less than 1 m on either side of the pods. The two GPS antennas collect normal GPS signals from the satellite constellation and correction signals from the John Chance network.*

For the June expedition, the barbed wire on the inner fence was removed, but the fence posts were left in the ground. The Kiwi had to occasionally be driven around rough terrain and various posts in the exclusion area. The removal of the barbed wire inner fence permitted the Kiwi to get inside the fence and gather data close to the mound. However, the terrain of the GZ mound and the depression just northeast of the mound was considered too steep and the Kiwi was not driven over that area. The mound was assumed to be an area which would have to be excavated and removed regardless of the measured level of activity, so no concerted attempt was made to collect data over the mound. This produced a "hole" in the data which needed to be addressed in the data analysis. The extensive general data analysis procedures for the Kiwi data are described later in Section 5. The specific handling of the "hole" is described in Section 6.5.

4.6 Experiment #6 (June)—HPGe *In Situ* Measurements

This experiment was a check and verification of the Kiwi system during the June expedition. The Suburban system, described in Experiment #1, made more than 50 measurements of the ^{241}Am activity at various locations both inside the exclusion fence and around the periphery. In addition, two measurements were made in the plume which extends south of the exclusion area and one measurement was made at the revegetation site northeast of Double Tracks.

The majority of the 50 measurements were conducted to transect the site from south to north and from west to east passing through the GZ area. Since some additional time remained after these measurements were made, several additional measurements were conducted along the circular grid axes at 120°, 150°, 210°, and 240° to define the plume better in these directions.

4.7 Experiment #7 (June)—Hot-Piece Activity Measurements

This experiment was intended to measure the total ^{241}Am activity on several of the chunks of material found by either the ATV system or by technicians using hand-held FIDLERs or spotting them visually while walking around. This debris appeared to be metallic pieces from the explosion with some surface Pu contamination. Several of these pieces were weighed, photographed, and measured for activity

piece were measured and an effective activity value determined.

In addition to the metallic debris, soil samples collected from the hottest areas within the inner fence were also measured. The soil was placed inside plastic bottles approximately 5 cm (2 in) in diameter and 15 cm (6 in) tall. Measurements were made from each side of the bottle and an effective activity value determined.

5.0 DATA REDUCTION PROCEDURES

Several methods for processing the Kiwi data may be employed. The gross count rate method calculates the total counts from all gamma rays detected during each one-second sample and presents the results as a series of equal-count-rate contours superimposed on a map or photograph of the survey area. With this display, large-scale variations of the radiation field within the whole survey area may be easily seen. Since the size of the Double Tracks survey area is relatively small and there are no real variations in the geology of the area, the gross count plot is quite flat—except in areas containing Pu contamination.

Variations in the total radiation field are not always of interest. At Double Tracks, the major contaminant is Pu (and its gamma-ray-emitting daughter Am). With this knowledge, the count rate in the ^{241}Am photopeak can be plotted versus position and a more sensitive plot of the contamination can be made from the isotopic count rate.

The main data reduction interest for this survey was the isotopic stripping of the ^{241}Am photopeak. The gross count rate method was principally a check to ensure that the data from adjacent "flights" matched each other and to provide a picture of the overall radiation field in the survey area.

5.1 Gross Count Rate Algorithm

The gross count rate is the sum of the counts in the energy range from 38 keV to 3,026 keV, divided by the live time, and subtracting a background term which represents all nonterrestrial sources.

$$C_G = \left(\frac{1}{t_{Live}} \sum_{E=38}^{3026} c(E) \right) - C_N \qquad (2)$$

where

C_G = gross count rate at the height of the detector (counts/s)

t_{Live} = live time during collection of gamma-ray spectrum (s)

$c(E)$ = the counts in the energy spectrum at the energy E (counts)

C_N = the count rate attributable to nonterrestrial sources (counts/s)

The lower energy limit is an effective lowest energy which the detector system can reliably record. Although the detector system processes and records all detected gamma rays up to 4,000 keV, there are almost no gamma rays of interest with energies above 3,000 keV, and the higher energies are generally ignored. The total number of counts attributable to nonterrestrial sources includes gamma rays emitted by airborne Rn and its daughters, cosmic rays, and vehicle and equipment contributions.

5.2 Isotope Extraction Algorithms

Before describing these windowing techniques, a few points need to be made about the energy spectrum. In general, the gamma rays emitted by naturally occurring radioisotopes have very precise, well-defined energies. If the gamma rays could be measured ideally, the energy spectrum would consist of very tall, very narrow photopeaks centered at the total energy of the gamma ray. (Some of the peaks would be riding on top of the slowly varying distribution of Compton-scattered gamma rays from other isotopes, but the peaks would be narrow.) However, the detector and associated electronics used to measure the gamma rays have energy resolutions which broaden the photopeak distribution. The spectrum actually recorded by the measuring system will have broader, Gaussian-shaped peaks with widths equal to the resolution of the detection system.

The total number of counts contained in the Gaussian-shaped photopeak can be obtained by summing all of the counts within a specific energy range, ΔE, of the gamma-ray energy, E. The magnitude of ΔE will determine the fraction of the total counts which are summed. If $\Delta E = 3\sigma$, where σ is the standard deviation of the Gaussian distribution, then 99.7% of the total photopeak counts will be included in the sum. This is not an unreasonable assumption for HPGe detectors, which have very narrow peak shapes. However, if the standard deviation for the system is large, as is the

case for NaI detectors, then the distributions from different photopeaks can overlap significantly. This interference between peaks can be minimized by decreasing ΔE, with the knowledge that not all of the counts will be included in the sum. A correction factor, determined in a region free of conflicting peaks, can be found to relate the number of counts in the range $E \pm \Delta E$ to the total counts in the peak.

5.2.1 Two-Window Algorithm

The two-window algorithm is the simplest of several window algorithms in use. It employs a narrow window centered on the energy of the specific photopeak. A background window, located at higher energies, assumes that the background counts in the photopeak window are proportional to the total counts recorded in the background window. The background window may abut the photopeak window or may be separated from it in energy. The equation for the two-window algorithm follows:

$$C_{2-Window} = \sum_{E=E_1}^{E_2} c(E) - K_2 \sum_{E=E_3}^{E_4} c(E) \qquad (3)$$

with

$$K_2 = \frac{\sum_{E=E_1}^{E_2} c_{bkg}(E)}{\sum_{E=E_3}^{E_4} c_{bkg}(E)} \qquad (4)$$

where

$C_{2\text{-}Window}$ = the net counts in the photopeak from the two-window algorithm

$c(E)$ = the counts in the gamma-ray energy spectrum at the energy E

E_n = the limiting energies of the windows ($E_1 < E_2 \leq E_3 < E_4$)

K_2 = the ratio of the counts in the photopeak window to the counts in the background window in a clean region of the survey area

$c_{bkg}(E)$ = the counts in the gamma-ray energy spectrum at the energy E in a clean region of the survey area

The proportionality factor, K_2, is determined in a region of the survey which does not contain any of the specific isotope, so that the photopeak window contains only its background counts and therefore is directly related to the number of counts in the background window. If the principle source of background gamma rays in the photopeak window is from scattered gamma rays from photopeaks at higher energies, this is a reasonable assumption. If there are isotopes other than the one of interest with photopeaks in the photopeak window, this algorithm will likely fail.

5.2.2 Three-Window Algorithm

If a region free of the specific isotope cannot be found or if the composition of the other isotopes changes drastically between the clean region and the rest of the survey area, then a simple multiplicative factor will not relate the counts in the photopeak window to the counts in the background window. To solve this problem, the three-window algorithm employs a background window on each side of the photopeak window. (In this case, the two background windows abut the photopeak window in energy.) This algorithm assumes that, for any spectrum, the number of background counts in the photopeak window is linearly related to the counts in the two background windows. The equation for the three-window algorithm follows:

$$C_{3-Window} = \sum_{E=E_2}^{E_3} c(E) - K_3 \left[\sum_{E=E_1}^{E_2} c(E) + \sum_{E=E_3}^{E_4} c(E) \right] \qquad (5)$$

with

$$K_3 = \frac{\sum_{E=E_2}^{E_3} c_{bkg}(E)}{\sum_{E=E_1}^{E_2} c_{bkg}(E) + \sum_{E=E_3}^{E_4} c_{bkg}(E)} \qquad (6)$$

where

$C_{3\text{-}Window}$ = the net counts in the photopeak from the three-window algorithm

E_n = the limiting energies of the windows ($E_1<E_2<E_3<E_4$)

K_3 = the ratio of the counts in the photopeak window to the counts in the two background windows in a clean region of the survey area

The three-window algorithm is also very useful in extracting low-energy photopeak counts where the shape of the Compton-scatter contributions from other isotopes is changing significantly.

Both the two- and three-window algorithms were applied to the Double Tracks data. In this particular case, the three-window algorithm produced an output which was more stable with regard to statistical variations in the data set.

5.3 Gridding of Data

To produce most of the plots in this report, the Kiwi data were forced into a 9-m (30-ft) grid. Since the data were collected second-by-second, the speed of the vehicle was not constant, and the actual "flight" lines often covered the same ground, gridding was necessary for the later processing. Since the interest in the data is predominantly to determine the ^{241}Am activity over square areas of 10-m (33 ft) and 100-m (330-ft) size, the gridding does not significantly degrade the spatial resolution of the data.

Once the grid is constructed, all spectra whose positions lie inside a grid cell are summed and an average count rate is calculated for the center of the grid.

$$c_g\,(E, x_c, y_c) = \frac{1}{N} \sum_{i=1}^{N} c(E, x_i, y_i) \qquad (7)$$

where

$c_g(E, x_c, y_c)$ = the average number of counts in the gamma-ray spectrum at energy E at the center of the grid cell at location (x_c, y_c)

N = the number of data samples contained within the grid cell

$c(E, x_i, y_i)$ = the number of counts in the gamma-ray spectrum at energy E from the ith spectrum collected at location (x_i, y_i)

The uncertainty in the gridded data (σ_g) is roughly $1/\sqrt{N}$ of the uncertainty of one of the original measurements (σ).

5.4 Count Rate Conversion to Soil Activity Concentration

The conversion from the count rate measured by a detector system to the activity of the isotope in the soil depends on several factors involving the radiation source, the intervening material, and the detection system. These factors include (a) ground roughness, (b) the distribution of the isotope in or on the soil, (c) the energy of the gamma ray emitted by the isotope, (d) the air density, (e) the amount of moisture in the soil, (f) the sensitivity of the detector system to the incident radiation, (g) the geometry of the detector-source arrangement including the use of collimators, and (h) the amount of background radiation (principally cosmic rays, vehicle and equipment background, and airborne Rn) present.

The soil activity concentrations deduced from the Kiwi system count rate are based on a simple multiplicative factor. The Kiwi was parked over an area inside the fence, and the count rate was measured for several minutes. This was an area which produced a fairly high count rate on both the Suburban system and on a hand-held FIDLER detector. The activity in this same area was also recorded in a series of HPGe tripod system measurements. To within the accuracy in which the two systems could measure the activity of the same location, this technique ensures consistency between the activities measured by the Kiwi and tripod systems. The conversion from count rate to activity for the tripod systems has been used extensively in the past and is briefly outlined below. The major problem with the area used at Double Tracks was the nonuniformity of the activity distribution. As seen throughout the survey area, the Am was dispersed in clumps in the high activity areas. There were large variations (a factor of 2-3) between the five tripod measurements, indicating that the activity was concentrated in one or two areas.

5.4.1 Distribution of the Isotope in the Soil

Three basic types of vertical distributions are commonly observed in the course of radiological surveys. All of the models used in this work assume that extended sources are uniform in the horizontal directions. That is, the only variation in the concentration

of the isotope in the soil is with depth. The uniform distribution in the horizontal plane leads to results expressed in terms of an average value over the field-of-view of the detector.

The naturally occurring radioisotopes are distributed uniformly as a function of depth. The fallout from the aboveground nuclear tests in the 1950s and 1960s began as a surface distribution. That is, all of the radioactivity lies in a thin layer of material on the ground. After a number of years, as the radioactive material has a chance to migrate into the soil, the initial surface distribution evolves into an extended distribution which is usually modeled by an exponential function. The relaxation length for the exponential distribution is expressed as $1/\alpha$. For the Pu and Am dispersed over 30 years ago at Double Tracks, an exponential distribution is assumed.

$$S(z) = S_{E0}\, e^{-\alpha z} \qquad (8)$$

where

$S(z)$ = the activity concentration of the isotope at the depth z

S_{E0} = the activity concentration of the isotope at the surface of the soil

α = the inverse of the exponential relaxation distance

For the exponential distribution, the volume of soil from the surface down to a depth of $1/\alpha$ contains approximately 63% of the isotope's total activity. At depths of $2/\alpha$ and $3/\alpha$ the volume of soil contains approximately 86% and 95% of the total activity, respectively. (This is different from the percent of the isotope which can be measured from a detector above the ground. If the gamma-ray energy is small, then regardless of the vertical distribution of the isotope, only the gamma rays emitted from the nuclei near the surface will be able to reach the detector with their full energy.)

5.4.2 Derivation of the Conversion Factors

The conversion factors are determined by combining a laboratory measurement of the detector's efficiency to a given gamma-ray energy with a theoretical calculation of the gamma-ray flux arriving at the detector as a function of source distribution in the soil. The derivation of these equations is given in several previous reports (for example Reference 8) which are generally based on the assumptions and derivations in the work by Beck.[9]

The number of photopeak counts registered by the detector depends on the flux of gamma rays at the location of the detector and a quantity, which is designated as the effective detector area, A. Since the probability of a gamma ray depositing its full energy in the detector depends on the detector dimensions, orientation, and gamma-ray energy, the effective area is not easily calculable. Instead the effective area is measured in the laboratory and expressed as a zero-degree value, A_0, multiplied by a function, $R(\theta)$, which contains all of the angular response. The effective area is measured at 10° intervals and linear interpolation is applied between the measured values.

The measured photopeak count rate can be expressed as an integral over the factors for the source activity in the soil, the detector's effective area, the distance from source to detector, and the attenuation of the gamma rays by the intervening material (air and soil). Figure 4 presents a visual representation of the detector-source geometry.

$$C_p = \int_0^\infty \int_0^\infty \frac{S(z) A_0 R(\theta)}{4\pi d^2} e^{-\left(\frac{\mu}{\rho}\right)_a \rho_a d_a} e^{-\left(\frac{\mu}{\rho}\right)_s \rho_s d_s} 2\pi r\, dr\, dz \qquad (9)$$

where

C_p = the net photopeak count rate

$S(z)$ = activity per unit volume [(γ/s)/cm^3]

A_0 = the effective area of the detector at 0°

$R(\theta)$ = the angular response of the detector at the angle θ

$d = d_a + d_s$, the distance from the source element to the detector (cm)

$(\mu/\rho)_{a,s}$ = air or soil mass attenuation coefficient (cm^2/g)

$\rho_{a,s}$ = air or soil density (g/cm^3)

Before proceeding any further with the derivation, the isotopic distribution in the soil must be determined. If no soil samples are available to determine the distribution, a distribution is assumed. Knowledge of the particular isotope and some history of how it might have arrived at this location as discussed in Section 5.4.1 will determine the form of $S(z)$. For the remainder of this derivation, the exponential distribution (see Equation 8) will be assumed.

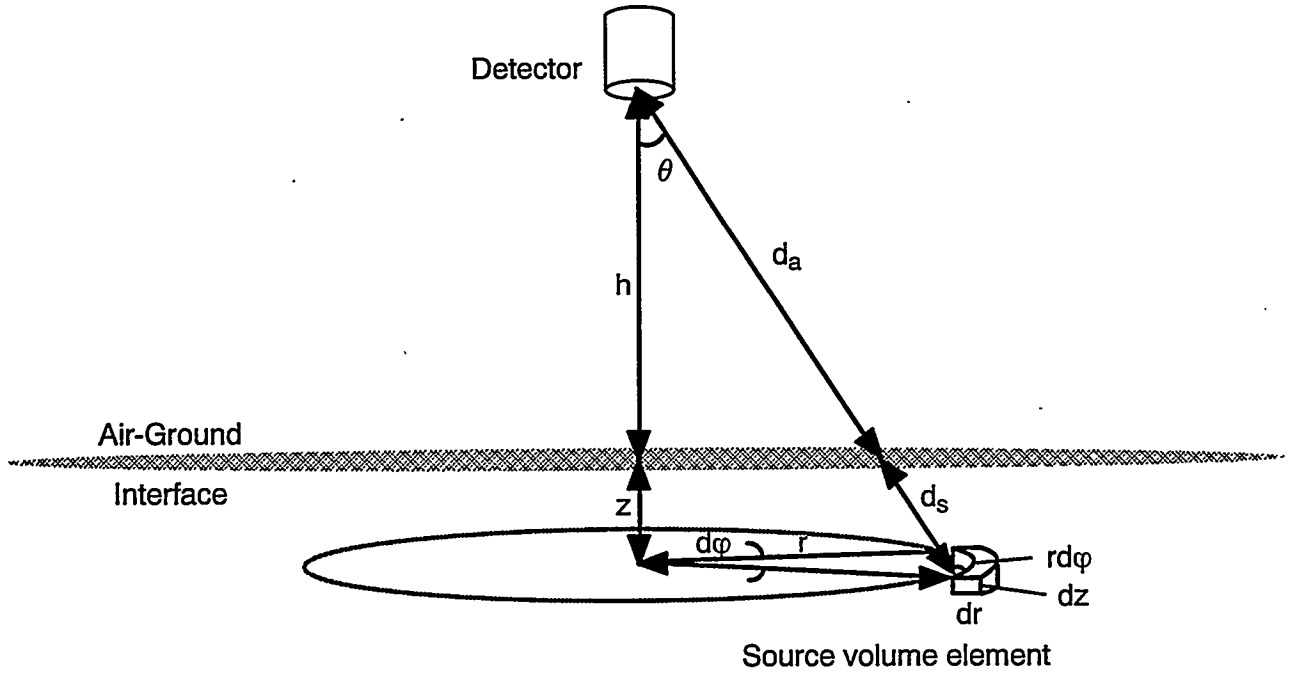

FIGURE 4. ***GEOMETRY FOR RADIATION MEASUREMENTS.*** *The detector-soil element geometry applies to both aerial and in situ measurements. The count rate of the detector results from the integrated gamma ray flux from all of the individual source elements.*

Following a change in the integration variables and for the exponential depth distribution, the count rate equation becomes

$$C_p = \frac{S_{E0}\, A_0}{2} \int_0^{\pi/2} \frac{R(\theta)\tan(\theta)\, e^{-\left(\frac{\mu}{\rho}\right)_a \rho_a h \sec(\theta)}}{\alpha + \left(\frac{\mu}{\rho}\right)_s \rho_s \sec(\theta)}\, d\theta \qquad (10)$$

5.4.3 Conversion Factors for Selected Isotopes in the Soil

The expression in Equation 10 relates the measured photopeak count rate, C_p, to the activity per unit volume at the surface, S_{E0}. The detector parameters, A_0 and $R(\theta)$, are usually obtained empirically for a given system using standard calibration sources. Mass attenuation coefficients for air and typical soils can be found in standard reference tables. An average soil density of 1.5 g/cm^3 is usually assumed unless actual measured values are available. The air density is calculated from measurements of the temperature and barometric pressure. The detector height, h, is measured and the inverse of the exponential relaxation length, α, is either measured or assumed. It is then a simple case of calculating the required integral numerically to obtain the conversion factor, F_E.

$$\frac{1}{F_E} = \frac{C_p}{S_{E0}} = \frac{A_0}{2} \int_0^{\pi/2} \frac{R(\theta)\tan(\theta)\, e^{-\left(\frac{\mu}{\rho}\right)_a \rho_a h \sec(\theta)}}{\alpha + \left(\frac{\mu}{\rho}\right)_s \rho_s \sec(\theta)}\, d\theta \qquad (11)$$

The conversion factor relates a measured photopeak net count rate, expressed in units of counts per second, to source activity at the surface expressed in units of gamma rays per second per unit volume. For a specific isotope, the source activity is generally changed to units of curies or becquerels. The average activity per unit volume can also be converted to average activity per unit mass by dividing by the soil density.

5.4.4 Average and Total Activity

When the interest is comparing the activity measured *in situ* with the activity obtained from a series of soil sample measurements, it is more useful to relate the photopeak net count rate data to an average concentration within a given soil depth rather than as the

exponential concentration at the surface. For a source distributed exponentially with depth, the average concentration in the top z_s is calculated with the following equation:

$$< S_{z_s} > = \frac{1}{z_s} \int_0^{z_s} S_{E0} e^{-\alpha z} dz = \frac{S_{E0}}{\alpha z_s} \left(1 - e^{-\alpha z_s}\right) \tag{12}$$

Soil samples generally collect all of the soil to a specific depth. The soil is taken to a laboratory where the contents of the sample are crushed and thoroughly mixed before a small quantity is analyzed. The above expression is valid for comparing the quantity of an exponentially distributed radioisotope measured by the *in situ* and the soil sample methods if the following two conditions are satisfied: (a) the concentration of the radioisotope at and below z_s is small compared to the quantity of the isotope at the surface and (b) the mean free path of the gamma ray is comparable to or larger than z_s. In other words, the comparison is only valid if the *in situ* measurement cannot measure any significant contribution from the radioisotopes below the cutoff depth, and it can measure all of the radioisotopes above the cutoff depth.

Another quantity often used when discussing exponentially distributed radioisotopes is the total activity per unit area. This represents all of the activity in an infinitely deep column of soil and is calculated with the following equation:

$$S_A = \int_0^{\infty} S_{E0} e^{-\alpha z} dz = \frac{S_{E0}}{\alpha} \tag{13}$$

The value of α is usually poorly known and is highly dependent upon the actual soil conditions and the isotopes which are present. Also, soil disturbance (farming, construction, etc.) will affect the relaxation depth. Variations in α can produce significant changes in the average activity.

6.0 DISCUSSION OF RESULTS

6.1 Experiment #1 (April)—HPGe *In Situ* Measurements

The ^{241}Am and TRU activity measurements made by the Suburban system are listed in Table 1 and shown in Figure 5 where the total activity is expressed in a similar manner to the previously processed aerial data except that the TRU:Am ratio is now 16:1 for both sets of data. The two "rows" of measurements in the southern half of the exclusion area are in the area where the aerial data showed fairly low, uniform activity. Also, several measurements were made in the general area east of the inner fence and along the road between the entrance and GZ.

Table 2 summarizes the results of the two hot-spot mining operations. The first mining area shows a reduction in the before-and-after 7.5-m (25-ft) height activity measurements by approximately a factor of 10 (file numbers 2 and 29). The change in activity in the 3-m (10-ft) AGL measurements is only about a factor of two (file numbers 3 and 30). The lower height measurement started with a much lower activity and did not see as large an area as the 7.5-m (25-ft) measurement, indicating that most of the hot pieces removed during the mining operation were outside this smaller field-of-view. The second mining location also had a fairly low activity, and even though several small pieces of material were found and removed, the effect of the mining operation wasn't sufficient at this location to overcome the uncertainties from the counting statistics in the 10-minute measurements.

6.1.1 Suburban Versus Tripod Measurements

Figures 6-8 (see pages 19 and 20) compare the ^{241}Am activities measured by the Suburban HPGe system operated at 3-m (10-ft) height and the tripod HPGe system operated at 1-m (3-ft) height. The first tripod grid location (see Figure 6) exhibits a relatively uniform, high ^{241}Am activity distribution with a slight increase in activity from the southeast corner to the northwest corner. The Suburban measurement agrees quite well with the individual tripod measurements.

The second grid location (see Figure 7) shows a dramatic increase in ^{241}Am activity from the west side to the east side, and the Suburban measurement seems to be excessively high compared to the tripod measurements. This may be the result of one or more hot pieces just on the edge of the Suburban field-of-view but outside the tripod system field-of-view. The circles are a rough indication of the field-of-view of the detector but may not be exactly to scale.

The third grid location (see Figure 8) shows a very hot area in the center of the grid with a much lower, nearly

Table 1. Suburban Measurements in April. The locations, Am concentrations, and TRU concentrations are shown for the HPGe measurements made at the Double Tracks area. The TRU concentration is based on a ($^{239}Pu + ^{240}Pu + ^{241}Am$): ^{241}Am ratio of 16. Positions shown in *italics* never received a lock on the differential GPS signal, so they have a positional uncertainty on the order of 100 m.

File No.	Latitude (N)	Longitude (W)	^{241}Am (pCi/g)		TRU (pCi/g)	
2	*37°42'17.97"*	*116°59'18.28"*	24.43	± 0.68	390.9	± 10.9
3[a]	37°42'17.92"	116°59'18.09"	3.12	± 0.44	49.9	± 7.0
4	37°42'13.48"	116°59'19.99"	33.55	± 0.77	536.8	± 12.3
5[a]	37°42'13.33"	116°59'19.62"	39.55	± 0.73	632.8	± 11.7
6	37°42'13.48"	116°59'21.16"	3.09	± 0.54	49.4	± 8.6
7	37°42'10.11"	116°59'22.96"	< MDA[b]		< MDA[b]	
8	37°42' 9.47"	116°59'21.30"	6.88	± 0.58	110.1	± 9.3
9[a]	37°42' 9.53"	116°59'21.11"	5.26	± 0.48	84.2	± 7.7
10	37°42' 9.13"	116°59'19.81"	20.13	± 0.67	322.1	± 10.7
11[a]	37°42' 9.20"	116°59'19.90"	15.89	± 0.56	254.2	± 9.0
12	37°42'13.37"	116°59'19.65"	38.33	± 0.78	613.3	± 12.5
22	37°42'19.90"	116°59'15.43"	3.65	± 0.54	58.4	± 8.6
23	37°42'20.67"	116°59'15.74"	7.61	± 0.59	121.8	± 9.4
24	37°42' 9.47"	116°59'20.92"	8.22	± 0.58	131.5	± 9.3
25	37°42' 8.96"	116°59'18.20"	< MDA[b]		< MDA[b]	
26	37°42' 8.89"	116°59'16.34"	< MDA[b]		< MDA[b]	
27	*37°42'12.62"*	*116°59'15.22"*	< MDA[b]		< MDA[b]	
28	*37°42'13.61"*	*116°59'18.20"*	< MDA[b]		< MDA[b]	
29	*37°42'17.82"*	*116°59'17.43"*	2.31	± 0.77	37.0	± 12.3
30[a]	*37°42'17.71"*	*116°59'16.87"*	1.79	± 0.66	28.6	± 10.6
31	*37°42'20.34"*	*116°59'14.36"*	3.91	± 0.76	62.6	± 12.2
32	*37°42'21.10"*	*116°59'16.26"*	23.31	± 0.98	373.0	± 15.7
33[a]	*37°42'20.07"*	*116°59'16.02"*	9.07	± 0.73	145.1	± 11.7
34	*37°42'10.31"*	*116°59'20.50"*	6.72	± 0.81	107.5	± 13.0
42	*37°42'20.42"*	*116°59'15.40"*	8.57	± 0.58	137.1	± 9.3
43	*37°42'22.16"*	*116°59'15.87"*	15.51	± 0.63	248.2	± 10.1
44	*37°42'21.03"*	*116°59'13.64"*	< MDA[b]		< MDA[b]	
45	*37°42'23.99"*	*116°59'14.92"*	5.58	± 0.56	89.3	± 9.0

[a] Measurements made at a height of 3 m versus the normal 7.5 m.

[b] The Minimum Detectable Activity (MDA) is equal to 3σ where σ is the standard deviation of the counting statistics. For measurements made at a height of 3 m, the MDA is 1.0 pCi/g of ^{241}Am and 16.0 pCi/g of TRU. For measurements made at a height of 7.5 m, the MDA is 1.5 pCi/g of ^{241}Am and 24.0 pCi/g of TRU.

uniform concentration around the edge. Here the Suburban measurement appears to be close to an average of the individual tripod measurements, as would be expected if the Suburban detector averages the inner hot spot over its full field-of-view. From these three grid measurements, it is clear that the Am

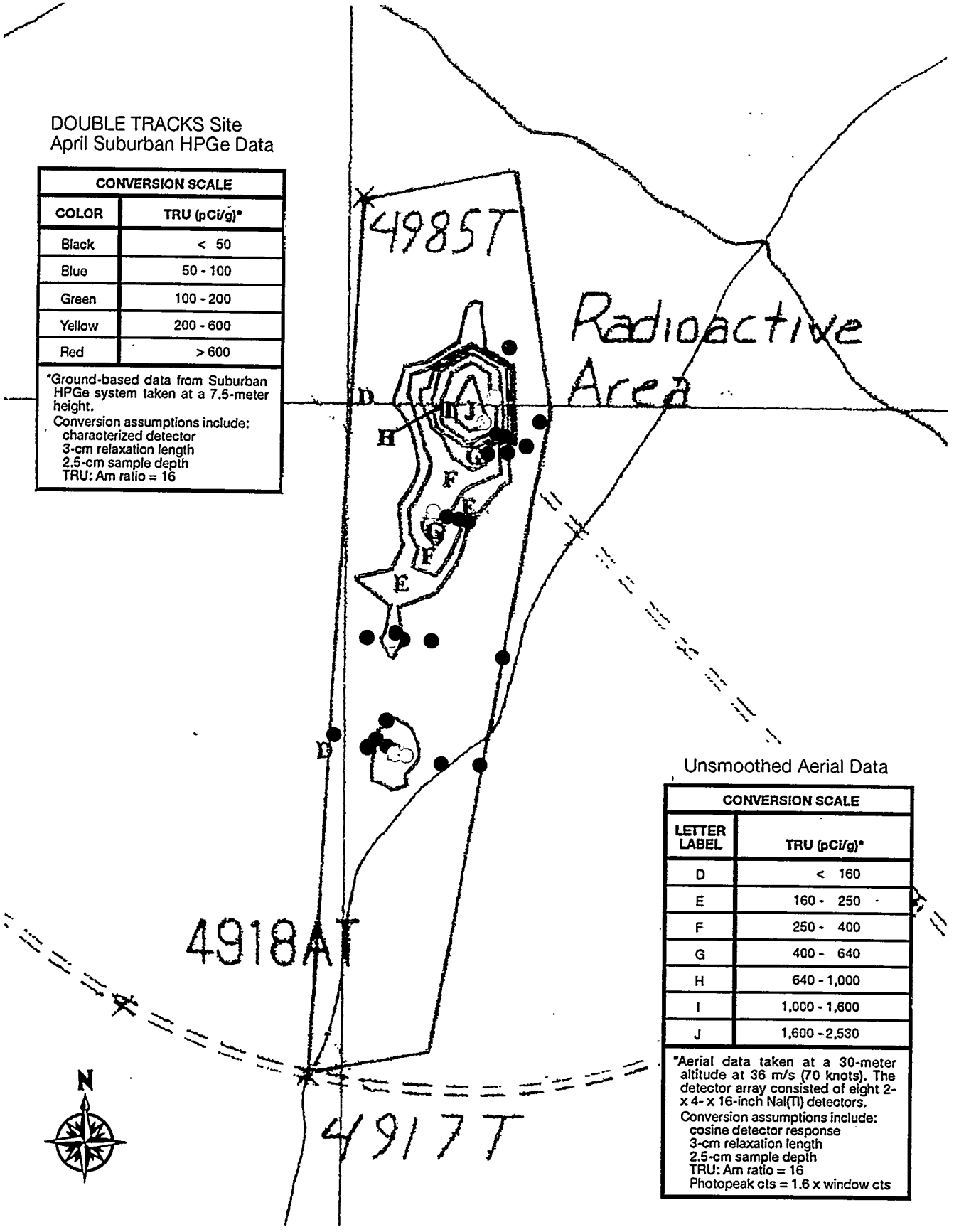

FIGURE 5. ***MEASUREMENT LOCATIONS OF THE SUBURBAN SYSTEM (APRIL).*** *The locations (by GPS coordinates) of the Suburban measurements are marked by colored dots corresponding to five bands of TRU activity. The contour data from the 1993 aerial survey are included for reference. Both sets of data use the 16:1 TRU:^{241}Am activity ratio.*

Table 2. "Mining" Location Measurements. The locations and Am concentrations are shown for the HPGe measurements made at the hot-spot mining areas. The TRU concentration is based on a (^{239}Pu + ^{240}Pu + ^{241}Am) : ^{241}Am ratio of 16. Positions shown in *italics* never received a lock on the differential GPS signal, so they have a positional uncertainty on the order of 100 m (300 ft). The Suburban could easily return to the same location to make the before-and-after measurements. However, knowing its absolute position relative to latitude and longitude is where the positional uncertainty lies. The positions are provided principally to relate this data with the aerial and Kiwi data shown in the later figures.

File No.	Latitude (N)	Longitude (W)	^{241}Am (pCi/g)		TRU (pCi/g)	
First mining location (7.5-m height)						
2	*37°42'17.97"*	*116°59'18.28"*	24.43	± 0.68	390.9	± 10.9
29	*37°42'17.82"*	*116°59'17.43"*	2.31	± 0.77	37.0	± 12.3
First mining location (3-m height)						
3	37°42'17.92"	116°59'18.09"	3.12	± 0.44	49.9	± 7.0
30	*37°42'17.71"*	*116°59'16.87"*	1.79	± 0.66	28.6	± 10.6
Second mining location (7.5-m height)						
22	37°42'19.90"	116°59'15.43"	3.65	± 0.54	58.4	± 8.6
31	*37°42'20.34"*	*116°59'14.36"*	3.91	± 0.76	62.6	± 12.2

distribution varies dramatically over distances of several meters (comparable to the fields-of-view of these detector systems).

6.1.2 Measurements South of the Exclusion Fence

Figure 9 (see page 21) shows the tripod measurements made south of the fence. Using the intersection of an arc road with an arroyo as a reference point (marked "REF." in figure), it was possible to establish the position and direction of the actual survey line after the measurements were completed. Measurements were made at distances of 6, 230, 460, 690, and 910 m (20, 750, 1,500, 2,250, and 3,000 ft) south of the fence. At the 910-m distance, measurements were made in an east and west direction at distances of 46 and 91 m (150 and 300 ft). The aerial data shown in this figure has been averaged over nine neighboring data points to produce a map of the lowest possible detectable activity of ^{241}Am.[5]

In comparing the data, it is important to take into account the difference in the area measured by each system. The *in situ* detector, mounted on a short tripod only 56 cm (22 in) above the ground, provides an average concentration value over an area approximately 5 m (15 ft) across. The 9-point neighbor averaged aerial data, taken at a survey altitude of 30 m (100 ft) and a 46-m (150-ft) grid spacing, provides an average concentration value over an area about 150 m (500 ft) in diameter. Near the fence, the *in situ* data shows higher levels than indicated by the aerial data. This would indicate that the width of the plume at this location is smaller than the field-of-view of the aerial system. The aerial system would show a narrow plume as covering a larger area but at a lower concentration value than actually exists on the ground. Further out from the fence, the two sets of data agree better. This would indicate that the plume is more dispersed and covers a wider area here than closer to the fence.

Both sets of data in Figure 9 used an assumed Pu:Am ratio of 10. Measurements made in April, as well as theoretical calculations, indicate that this value is too low. As discussed in this report, a value of 16 will be used for the total alpha-emitting TRU:Am ratio for this site. Therefore, all data in Figure 9, both aerial and ground-based, should be multiplied by 1.6 before comparing to TRU data presented elsewhere.

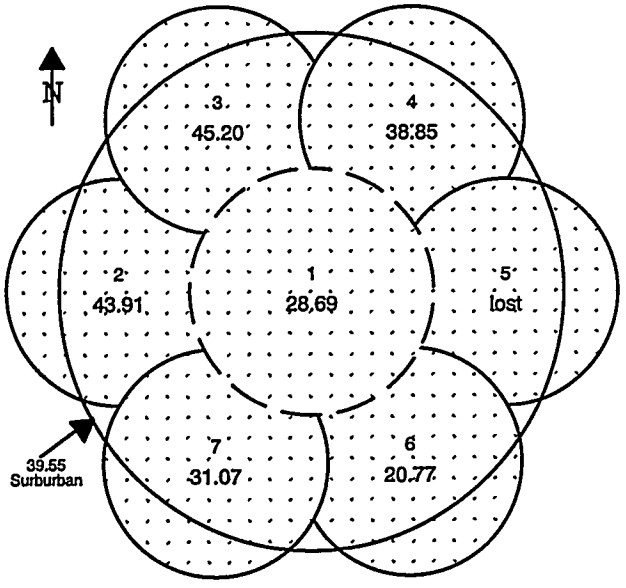

Surburban File #5: First Tripod Grid

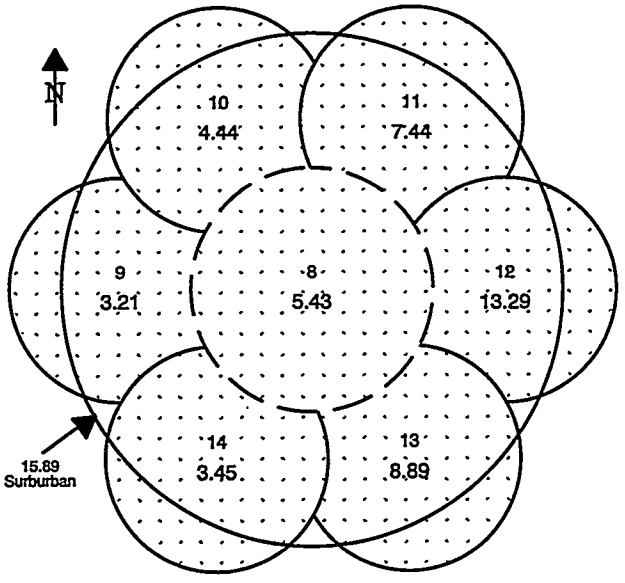

Surburban File #11: Second Tripod Grid

FIGURE 6. ***SUBURBAN VERSUS TRIPOD MEASUREMENTS—FIRST LOCATION.*** *The ^{241}Am soil activity concentrations (pCi/g) as measured by the Suburban HPGe detector at a 3-m height versus the tripod detector measurements at 1-m height. Note the general increase in activity from the southeast corner to the northwest corner. Data from footprint #5 was inadvertently not written to tape and the omission was not detected until after the survey team had left the field.*

FIGURE 7. ***SUBURBAN VERSUS TRIPOD MEASUREMENTS—SECOND LOCATION.*** *The ^{241}Am soil activity concentrations (pCi/g) as measured by the Suburban HPGe detector at a 3-m height versus the tripod detector measurements at 1-m height. Note the dramatic increase in activity from west to the east.*

6.1.3 Highest Concentration of TRU Activity

As discussed in the next section, two different HPGe detectors made measurements on the mound to assess the Pu:Am ratio. Although the experiments were designed for the less stringent requirement of calculating the Pu:Am ratio, the activity of the soil on the mound can be deduced from these measurements if a few more assumptions are included.

The first detector system made measurements in both collimated and uncollimated arrangements. The uncollimated measurements should be ignored since the detector could see a significant amount of area away from the mound. The collimated measurements provide a more accurate measurement of only the soil on the mound and produce an ^{241}Am activity in the range 1,900-2,800 pCi/g, depending on the assumption of the depth to which the Am is distributed. The second detector system had a slightly different collimation arrangement and deduced an activity of about 2,500 pCi/g. Multiplying these numbers by the TRU:Am ratio of 16:1 yields a TRU activity of 30,000-45,000 pCi/g for the first system and 40,000 pCi/g for the second system. Since TRU waste is defined as having a total activity greater than 100,000 pCi/g (see DOE Order 5820.2A), the hottest portion of the mound does not exceed this level (when averaged over the field-of-view of the tripod system).

During the June expedition (see Section 6.7), measurements of individual 300-800-g soil samples from the mound and surrounding area produced TRU activities of 100,000-800,000 pCi/g. The HPGe detectors viewed an area of ground much larger than these soil samples and, as observed throughout the two expeditions, the Pu and Am contamination is not dispersed in a uniform pattern.

The activity results are close enough to the TRU limit that several ideas were proposed to ensure that the total activity of any truckload of soil removed from the Double Tracks site would not exceed the TRU limit. One of the principal means of reducing the total activity of the soil was to remove the hot pieces coated with Pu. This would make a small amount of TRU, but the

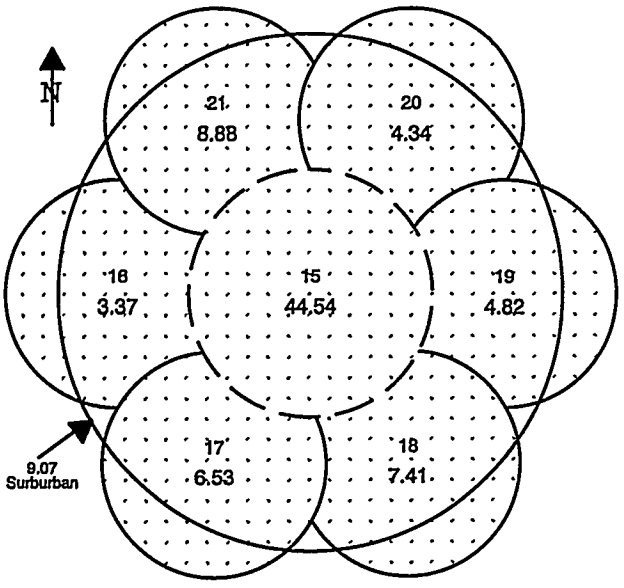

FIGURE 8. ***SUBURBAN VERSUS TRIPOD MEASUREMENTS—THIRD LOCATION.*** *The ^{241}Am soil activity concentrations (pCi/g) as measured by the Suburban HPGe detector at a 3-m height versus the tripod detector measurements at 1-m height. Note the high concentration only in the center of the figure with the outer circles having much less.*

many truckloads of soil would certainly be below the limit. This desire to locate the hot pieces and the success of the "mining" of the hot spots found with the hand-held FIDLER detectors were the major impetus behind the ATV hot-spot search in June.

6.2 Experiment #2 (April)—Pu:Am Ratio Measurements

For the two methods of measurement, the analysis was performed independently. The ratio calculation is based on measuring the 60-keV gamma rays emitted by ^{241}Am and three of the gamma rays emitted by ^{239}Pu (129 keV, 375 keV, and 414 keV). Within statistical uncertainties, the ratio of the Am activity relative to the Pu activities calculated from each of its gamma rays should be the same. There are differences in the activities of the two methods, principally as a result of different assumptions about the source-depth distribution, counting statistics, detector characterization, etc. As noted earlier, the attempt to measure the 39- and 51-keV X-rays from ^{239}Pu was unsuccessful, as the large Compton background from the ^{241}Am gamma rays nearly obliterated these X-ray peaks.

The results of the first method of measuring this ratio are presented in Table 3 (see page 22). A relaxation length of 20 cm (8 in) was assumed for the vertical distribution of ^{241}Am. The top portion of the table presents the average activity levels for the three sampling depths of 2.5, 5, and 20 cm. Only the longest time measurements for each arrangement are shown since the only change is a very slight improvement in counting statistics with the increasing time of the measurement. The Pu:Am ratio and the uncertainty in this ratio (based only on the counting statistics) are presented in the bottom portion of the table.

For the uncollimated data, the detector "sees" the Pu gamma rays from a larger area than it sees the Am gamma rays. Thus the Pu activities and the Pu:Am ratios for the uncollimated detector are too high. The collimators used in these measurements are very efficient at removing gamma rays at 60 keV but not as efficient at higher energies such as the gamma rays from ^{239}Pu. To reach the same fractional attenuation, about twice as much material (air, soil, Pb, etc.) is needed to attenuate the 129-keV gamma rays by the same fraction as the 60-keV gamma rays and about three times as much material for the 375- and 414-keV gamma rays. These measurements also are probably too high since a nontrivial fraction of the higher-energy Pu gamma rays can reach the detector after passing through the side of the collimator, while the Am gamma rays are completely attenuated.

Results for the second ratio measurement method, using the highly collimated HPGe detector, are given in Table 4 (see page 23) for both the 300- and 600-second measurements. Activity values, in pCi/g, are given for both Am and Pu, as determined from each individual gamma ray. The bottom of Table 4 shows the resulting ratios of ^{239}Pu:^{241}Am derived from each of the Pu gamma-ray lines. Ratios vary as a result of counting statistics in analyzing each gamma-ray photopeak, as well as the uncertainty in the depth distribution.

Table 5 (see page 24) shows the theoretical ratios due to decay from the original mixture of the Pu supposedly used in the test. Averaging the results from all three Pu gamma rays and from both the 300- and 600-second acquisitions leads to values of 14.91 ($1/\alpha$ = 3 cm), 12.36 ($1/\alpha$ = 20 cm), and 11.72 ($1/\alpha$ =

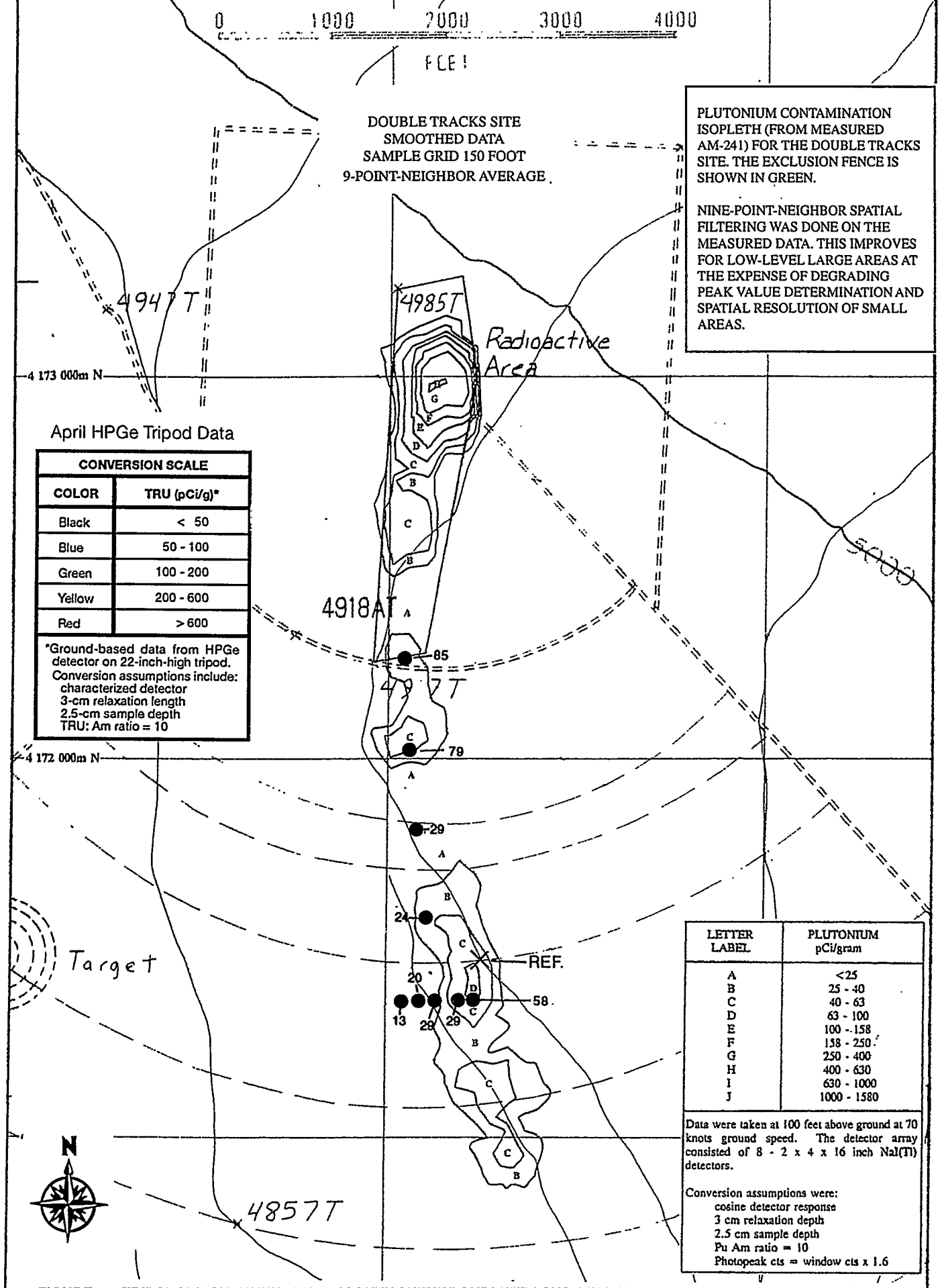

FIGURE 9. *TRIPOD MEASUREMENTS MADE SOUTH OF THE DOUBLE TRACKS FENCE (APRIL). Nine HPGe measurements from the April expedition are superimposed on the smoothed aerial data from December 1993. Both sets of data use the same Pu:Am ratio of 10:1, which is different from the rest of the data and figures presented in this report.*

Table 3. Pu:Am Ratio Measurements for the First Method. The Pu:Am ratio is an average of the ratios based on the 60-keV ^{241}Am photopeak and three of the gamma-ray photopeaks from ^{239}Pu. Since these measurements were made on the mound near GZ, the calculations in this table assume a nearly uniform depth distribution (exponential distribution using a relaxation length of 20 cm [8 in]). Activity results for three different sampling depths are presented; the ratio calculations do not depend on the sampling depth.

	Uncollimated (1800 s) Sampling Depth (cm)			Collimated (3000 s) Sampling Depth (cm)		
	2.5	5	20	2.5	5	20
Average activity (pCi/g)						
60 keV	1,925	1,812	1,294	2,820	2,654	1,896
129 keV	32,669	30,750	21,968	42,797	40,283	28,779
375 keV	29,601	27,862	19,906	36,780	34,619	24,733
414 keV	31,381	29,538	21,102	34,774	32,731	23,384
Pu:Am ratios for each ^{239}Pu gamma ray relative to ^{241}Am						
	Ratio	**Uncertainty**		**Ratio**	**Uncertainty**	
129 keV	16.97	±0.24		15.18	±0.24	
375 keV	15.38	±0.51		13.04	±0.54	
414 keV	16.30	±0.57		12.33	±0.56	
Average	**16.21**	**±0.81**		**13.52**	**±0.86**	

100 cm). These results are in general agreement with the theoretical prediction of 12.53 from Table 5. The results show closer agreement for the deeper depth distributions, which are more likely in the case of contamination within the mound soil. Based on these results, the information presented in Table 5 should provide a reasonable estimate for the appropriate ratio data.

In analyzing risk associated with Pu contamination in soil, it is usual to include activity levels of all significant alpha-emitting isotopes. Alpha emitters are of most concern since inhalation into the lungs is the path leading to the highest potential dose from Pu-contaminated soil. For Pu contamination, the isotopes of concern are ^{239}Pu, ^{240}Pu, and ^{241}Am. These are usually combined and referred to as the total TRU alpha emitters.

Table 5 gives a $^{239\text{-}240}$Pu:^{241}Am ratio of 100/7.291645 = 13.71 which, when the Am is added, yields a TRU:^{241}Am ratio of 14.71. Due to potential differences in migration of Pu and Am in the soil, the actual *in situ* ratio may vary somewhat from the theoretical prediction. In order to account for potential uncertainties in the actual ratio currently existing at Double Tracks, a value of 16 is recommended for use in determining concentration values from the ^{241}Am measurements. This is approximately 10% higher than the theoretical prediction and provides a reasonable margin of error for uncertainties in the actual ratio.

6.3 Experiment #3 (April)—Depth Profiling Measurements

6.3.1 Side Wall Measurements with TLD Material

Of the three measurements made near the inner fence, the first two were in areas that showed little or no elevated activity with a FIDLER. The FIDLER measurements were not made until after the first two sets of TLD material had been placed. As expected, results from these sheets showed basically background activity. The third set was placed in an area of elevated activity as identified with a FIDLER. The

Table 4. Pu:Am Ratio Measurements for the Second Method. The Pu:Am ratio is an average of the ratios based on the 60-keV ^{241}Am photopeak and three of the gamma-ray photopeaks from ^{239}Pu. These measurements were made with a highly collimated HPGe detector placed on the mound at GZ. Activity values and the corresponding ratios for three different relaxation lengths are presented.

	300 Second Data Relaxation Length (cm)			600 Second Data Relaxation Length (cm)		
	3	20	100	3	20	100
Average activity (pCi/g)						
60 keV	2,584	2,860	2,883	2,308	2,556	2,576
129 keV	36,826	36,360	35,544	40,442	39,930	39,035
375 keV	30,899	27,397	25,865	33,708	29,887	28,216
414 keV	39,620	34,689	32,606	36,343	31,820	29,909
Pu:Am ratios for each ^{239}Pu gamma ray relative to ^{241}Am						
129 keV	14.25	12.71	12.33	17.52	15.62	15.15
375 keV	11.96	9.58	8.97	14.60	11.69	10.95
414 keV	15.33	12.13	11.31	15.75	12.45	11.61
Average	**13.85**	**11.47**	**10.87**	**15.96**	**13.25**	**12.57**
Average of 300- and 600-second results				**14.91**	**12.36**	**11.72**

surface sheet showed several hot spots with most of the area exhibiting background levels. The vertical sheet also showed several hot spots but with no real continuum that would lead to a profile. One hot spot was found near the surface and another approximately 10 cm (4 in) below the surface. It is most likely that the hot spot below the surface was transported there by the shovel in trying to make the side wall to sample.

The TLD material is quite valuable for showing the distribution of activity with a very high spatial resolution (1mm [0.04 in]). For depth profile studies, however, the method used to form a side wall can influence the results. Similar conclusions were reached by ORNL in their attempt to use a track etch detector for measuring alpha contamination. Although in theory the technique should work, in practice, the direct HPGe measurement technique appears to be a better solution.

6.3.2 Comparison Between the Pu X-Rays and the ^{241}Am Gamma Ray

As expected based on the FIDLER readings, no Am activity was measured at the first two TLD measurement locations. The remaining sites showed the 60-keV gamma ray but no evidence of any X-rays. This included an extremely hot area near the mound which contained sufficient activity to allow direct measurements of the gamma rays from ^{239}Pu.

The lack of any X-rays likely resulted from three reasons: (a) the attenuation in soil, (b) the very small area actually being measured, and (c) the height of the detector above the ground. Because the collimator limited the field-of-view to a 10-cm- (4-in-) diameter circle, the actual amount of soil being measured was quite small. In addition, the detector was approximately 60 cm (24 in) above the ground. Even for the 60-keV gamma ray, only a weak signal was obtained in three of the four locations where elevated activity was measured. A better approach probably would have been to put the detector, with its sides collimated, right on the ground. This would have greatly increased the signal from the 60-keV gamma ray and might have shown the X-rays. This method definitely

Table 5. Pu:Am Ratio Calculations from Initial Composition. The Pu:Am ratio shown here is a simple decay of the Pu and Am isotopes in the initial composition. The ratio is shown as a percentage of Am:Pu, rather than as a Pu:Am ratio as in the rest of this report.

	^{238}Pu	^{239}Pu	^{240}Pu	^{241}Pu	^{242}Pu	^{241}Am	Total
Mol. Weight (g)	238	239	240	241	242	241	
Mass Fraction	3.9E-05	0.97314	0.0253	0.001487	3.1E-05	0	0.999997
Half Life (yrs)	87.75	24131	6569	14.4	376000	432	
Lambda (per yr)	0.007899	2.9E-05	0.000106	0.048135	1.8E-06	0.001605	
(Ci/g) of Pu + Am(t=0)	0.000662	0.0603	0.005735	0.153124	1.2E-07	0.000974	0.220795
Activity Fraction	0.002999	0.273102	0.025974	0.693513	5.5E-07	0.004411	

Note: All activities are nuclear transformation rates, not particle emission rates.

		Curies from 1 Ci of Pu+Am Mixture						^{241}Am: ^{239}Pu	^{241}Am: (^{239,240}Pu)
Time	Year	^{238}Pu	^{239}Pu	^{240}Pu	^{241}Pu	^{242}Pu	^{241}Am	% Activity Ratio	% Activity Ratio
0	1963	0.002999	0.273102	0.025974	0.693513	5.5E-07	0.004411	1.615281	1.475
1	1964	0.002976	0.273094	0.025971	0.660921	5.5E-07	0.00549	2.010224	1.835656
2	1965	0.002952	0.273087	0.025968	0.629861	5.5E-07	0.006516	2.385876	2.1787
3	1966	0.002929	0.273079	0.025965	0.600261	5.5E-07	0.007491	2.743144	2.504962
4	1967	0.002906	0.273071	0.025963	0.572052	5.5E-07	0.008418	3.082893	2.81523
5	1968	0.002883	0.273063	0.02596	0.545168	5.5E-07	0.0093	3.405947	3.110257
6	1969	0.00286	0.273055	0.025957	0.519548	5.5E-07	0.010139	3.713092	3.390759
7	1970	0.002838	0.273047	0.025954	0.495131	5.5E-07	0.010936	4.005075	3.657419
8	1971	0.002816	0.273039	0.025952	0.471863	5.5E-07	0.011693	4.282609	3.910889
9	1972	0.002793	0.273032	0.025949	0.449688	5.5E-07	0.012413	4.546376	4.151789
10	1973	0.002771	0.273024	0.025946	0.428554	5.5E-07	0.013097	4.797022	4.38071
11	1974	0.00275	0.273016	0.025944	0.408414	5.5E-07	0.013747	5.035165	4.598216
12	1975	0.002728	0.273008	0.025941	0.389221	5.5E-07	0.014364	5.261393	4.804844
13	1976	0.002707	0.273	0.025938	0.37093	5.5E-07	0.01495	5.476267	5.001106
14	1977	0.002685	0.272992	0.025935	0.353498	5.5E-07	0.015507	5.680321	5.18749
15	1978	0.002664	0.272985	0.025933	0.336885	5.5E-07	0.016035	5.874066	5.364461
16	1979	0.002643	0.272977	0.02593	0.321053	5.5E-07	0.016537	6.057985	5.532461
17	1980	0.002622	0.272969	0.025927	0.305965	5.5E-07	0.017013	6.232542	5.691913
18	1981	0.002602	0.272961	0.025924	0.291586	5.5E-07	0.017465	6.398178	5.84322
19	1982	0.002581	0.272953	0.025922	0.277883	5.5E-07	0.017893	6.555313	5.986765
20	1983	0.002561	0.272945	0.025919	0.264824	5.5E-07	0.018299	6.704346	6.122914
21	1984	0.002541	0.272938	0.025916	0.252379	5.5E-07	0.018684	6.845661	6.252015
22	1985	0.002521	0.27293	0.025913	0.240518	5.5E-07	0.019049	6.97962	6.374399
23	1986	0.002501	0.272922	0.025911	0.229215	5.5E-07	0.019395	7.10657	6.490384
24	1987	0.002481	0.272914	0.025908	0.218443	5.5E-07	0.019723	7.226841	6.600272
25	1988	0.002462	0.272906	0.025905	0.208177	5.5E-07	0.020033	7.340749	6.704348
26	1989	0.002442	0.272898	0.025903	0.198394	5.5E-07	0.020327	7.448593	6.802888
27	1990	0.002423	0.272891	0.0259	0.18907	5.5E-07	0.020605	7.550659	6.896152
28	1991	0.002404	0.272883	0.025897	0.180185	5.5E-07	0.020868	7.647219	6.984389
29	1992	0.002385	0.272875	0.025894	0.171717	5.5E-07	0.021117	7.738534	7.067836
30	1993	0.002366	0.272867	0.025892	0.163647	5.5E-07	0.021351	7.824851	7.146719
31	1994	0.002348	0.272859	0.025889	0.155957	5.5E-07	0.021573	7.906406	7.221254
32	1995	0.002329	0.272851	0.025886	0.148627	5.5E-07	0.021783	7.983423	7.291645
33	1996	0.002311	0.272843	0.025883	0.141643	5.5E-07	0.021981	8.056116	7.358089
34	1997	0.002293	0.272836	0.025881	0.134986	5.5E-07	0.022167	8.124691	7.420771
35	1998	0.002275	0.272828	0.025878	0.128642	5.5E-07	0.022343	8.189341	7.47987
36	1999	0.002257	0.27282	0.025875	0.122597	5.5E-07	0.022508	8.250252	7.535554
37	2000	0.002239	0.272812	0.025872	0.116835	5.5E-07	0.022664	8.307601	7.587985
38	2001	0.002222	0.272804	0.02587	0.111345	5.5E-07	0.022811	8.361555	7.637317
39	2002	0.002204	0.272796	0.025867	0.106112	5.5E-07	0.022948	8.412276	7.683696

did not work as implemented. A modified version might be successful if the activity is very shallow. There appears to be no reason for further work in this area as the probability of success seems quite low.

6.3.3 Direct HPGe Measurements

Although not providing as fine a spatial resolution as possible with the TLD material, this is a very simple technique for field use. Results from these measurements showed that most of the activity was in the top 2-4-cm (1-2-in) region with one location exhibiting activity down to 8 cm (about 3 in). This shallow distribution is typical of that found for Pu in undisturbed areas. Additional time should be spent developing optimum methods to remove soil in thin layers. (It took several attempts to consistently remove a thin layer of soil; the first several attempts were almost always too deep.) Some additional work should also be done to determine the best detector height and field-of-view combination. Assuming 5-minute measurements, this method can provide a good estimate of the depth of contamination within approximately 30 minutes. This is far superior to the time and cost of obtaining profile samples and analyzing them in a remote laboratory. The method would be more tedious, and likely not as successful, for contaminants that are distributed more deeply into the soil, such as ^{137}Cs from typical worldwide fallout.

6.4 Experiment #4 (June)—ATV Hot-Piece Search

The ATV system was very successful in locating small areas of elevated activity which could then be surveyed with hand-held FIDLER detectors to find the hot piece. No recordable data were collected with this system; this was strictly a search and mark experiment (although the miners were able to show that these small areas could be cleaned up). The search was conducted as a series of east-west paths and covered the area from a little more than 150 m (500 ft) south of GZ to about 60 m (200 ft) north of GZ.

Since the ATV hot-piece search and the Kiwi survey (below) were conducted in parallel, some of the pieces found and removed during the ATV search had been detected earlier by the Kiwi. Therefore the small hot spots within the above distance limits from GZ and present in the Kiwi plots shown later in this report should be considered as already removed during the ATV search and not as areas which need further cleanup.

6.5 Experiment #5 (June)—Kiwi Survey Measurements

The results of the Kiwi survey are displayed in Figures 10-13 (see pages 26-29). Figure 10 presents both the gross count and TRU activity levels on the original second-by-second locations. The ^{241}Am activity is calculated from each spectrum by extracting the net counts in a window around the 60-keV photopeak. The TRU activity is calculated from the ^{241}Am activity by multiplying by the TRU:^{241}Am ratio of 16:1 described in Section 6.2. In addition to the color-coded points, the "flight" lines traveled by the Kiwi vehicle are clearly traceable over most of the area.

The individual second-by-second measurements are displayed as small squares which, in this display, are just slightly smaller than the actual footprint of the measurement. The displayed squares are about 2 m (7-8 ft) in length. The detector footprint is closer to 3 m (10 ft) perpendicular to the direction of travel. Along the vehicle path, the detector footprint varies with the speed of the vehicle but, in any case, would provide continuous coverage of the ground along the direction of travel. Thus the only real gaps in the coverage are those between the flight lines. Where the flight lines intersect, it is not always easy from this display to separate which set of data belongs to which flight line.

Of major interest in Figure 10 is the large hole in the data as the Kiwi had to avoid driving over the mound and the small depression just northeast of the mound. In later analysis, a linear interpolation of the measured activity filled this gap. The main effect of the linear interpolation is that, in later plots, the hottest activity location appears just east of the mound rather than on top of it. Other instrument surveys (mainly hand-held FIDLERs) indicated higher activity just east of the mound, although their results were not recorded.

Figure 11 shows the results of collecting all of the individual second-by-second measurements into a nominal 9-m (30-ft) grid and averaging the data over this interval. This plot presents the gross count data which is simply a sum of all of the gamma rays detected in each spectrum. As expected for a region this small, the gross count activity outside the area of actual contamination is quite uniform (varying by only 5%). The lack of data over the mound and the resulting linear interpolation caused the highest contour level to appear over the flight line closest to the mound on the

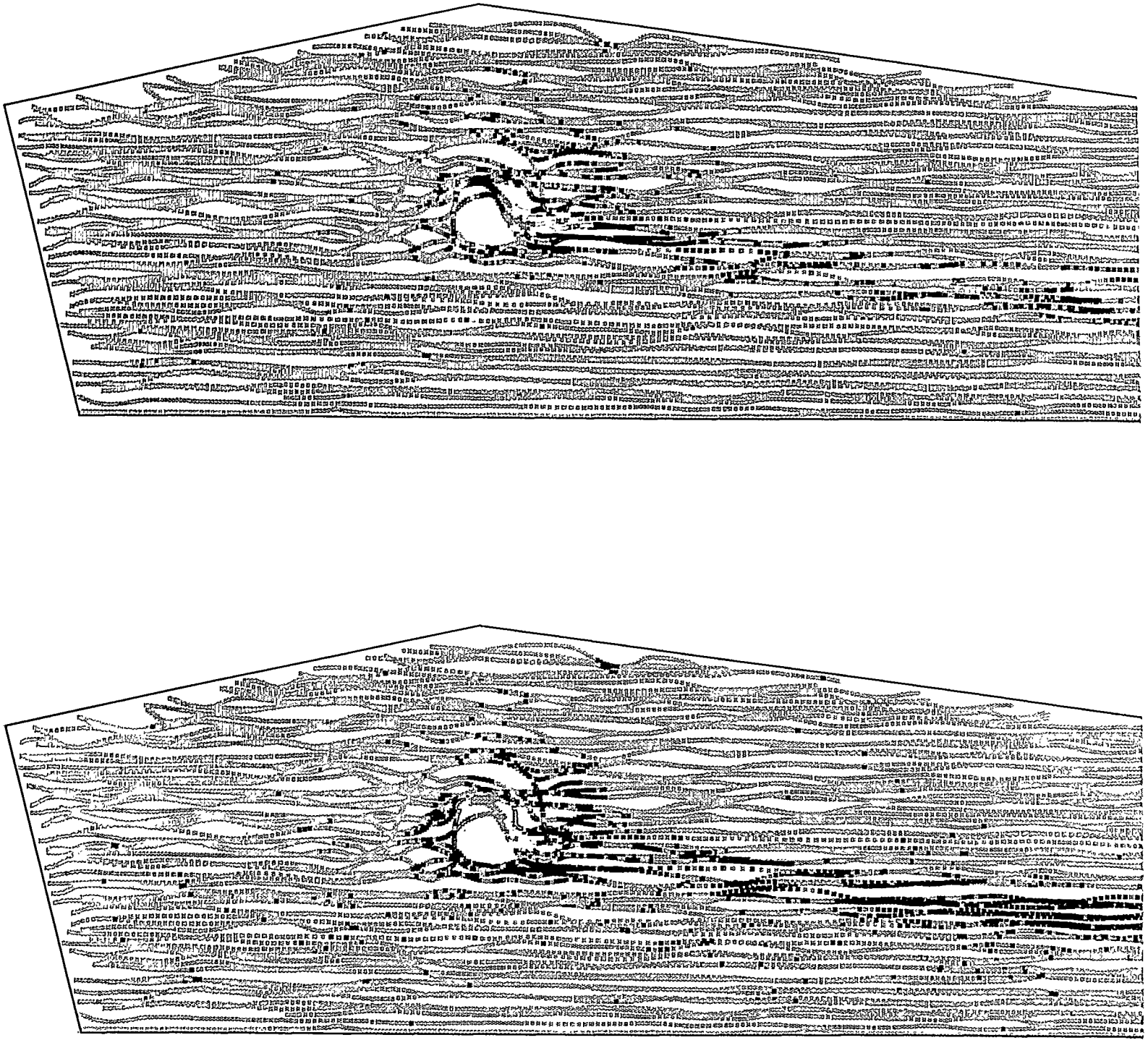

FIGURE 10. ***KIWI POINT-BY-POINT GROSS COUNT AND TRU ACTIVITY LEVELS:*** *The data collected by the Kiwi system each second are presented with different colors corresponding to the different gross count and TRU activity levels. The TRU:^{241}Am ratio is 16:1. Each square represents an individual measurement of the activity; the size of the square is about the width of the detector's footprint.*

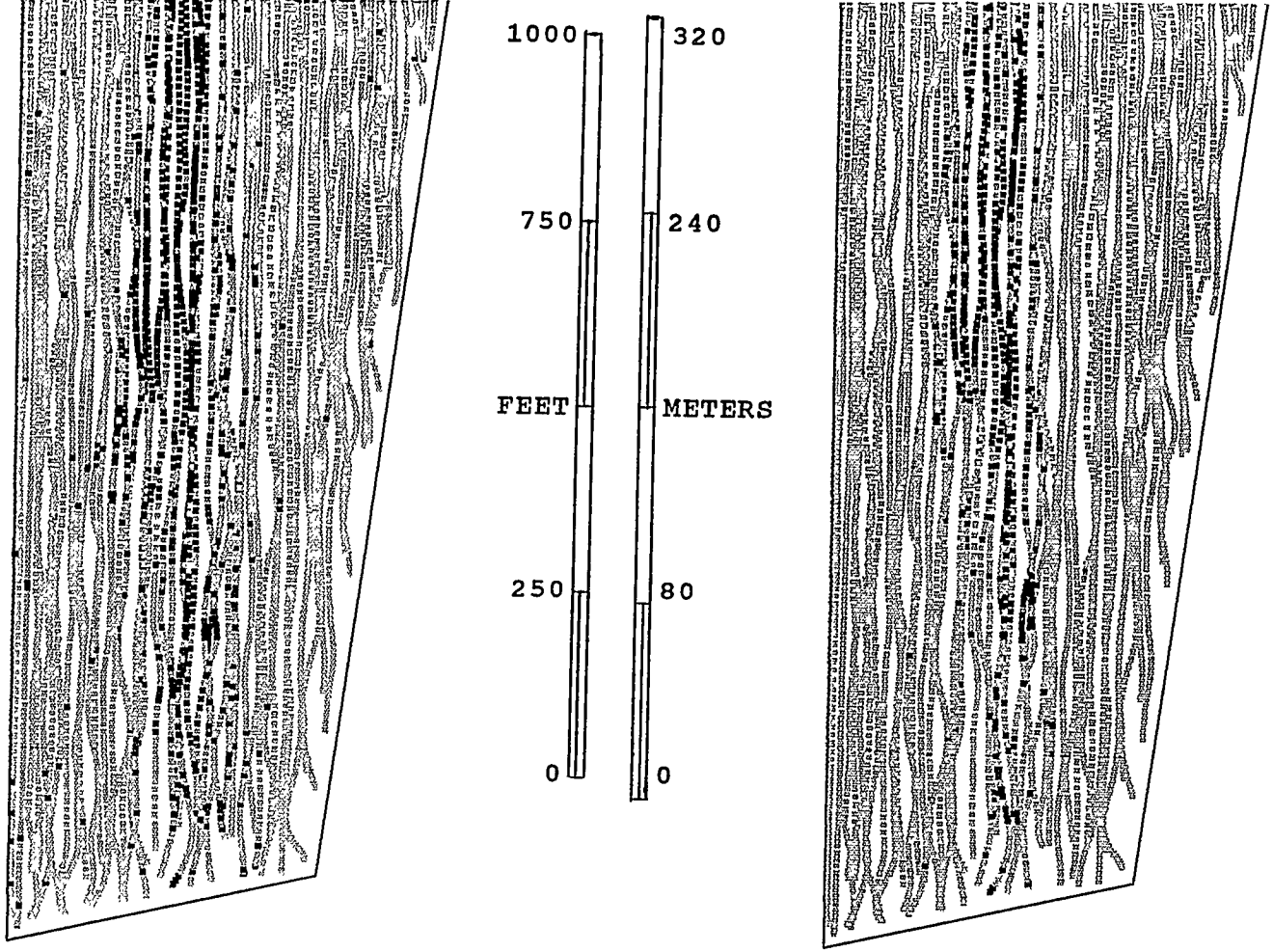

OBSERVED GROSS COUNTS PER SECOND
(40 keV THROUGH 3026 keV, SECOND BY SECOND)

		GRAY	<	18000
18000	<	LT BLUE	<	19000
19000	<		<	20000
20000	<	LT GRN	<	21000
21000	<	GREEN	<	24000
24000	<	YELLOW	<	33000
33000	<	ORANGE	<	60000
60000	<	PINK	<	140000

TOTAL TRANSURANIC PICOCURIES/GRAM
(FROM 3 WINDOW AM-241, SECOND BY SECOND)

		GRAY	<	50
50	<	LT BLUE	<	100
100	<		<	200
200	<	LT GRN	<	400
400	<	GREEN	<	800
800	<	YELLOW	<	1600
1600	<	ORANGE	<	3200
3200	<	PINK	<	6400
6400	<		<	12800
12800	<		<	25600

NAFR DOUBLE TRACKS "KIWI" DATA - JUNE 1995

MAP PRODUCED 10/6/95 EG&G/EM

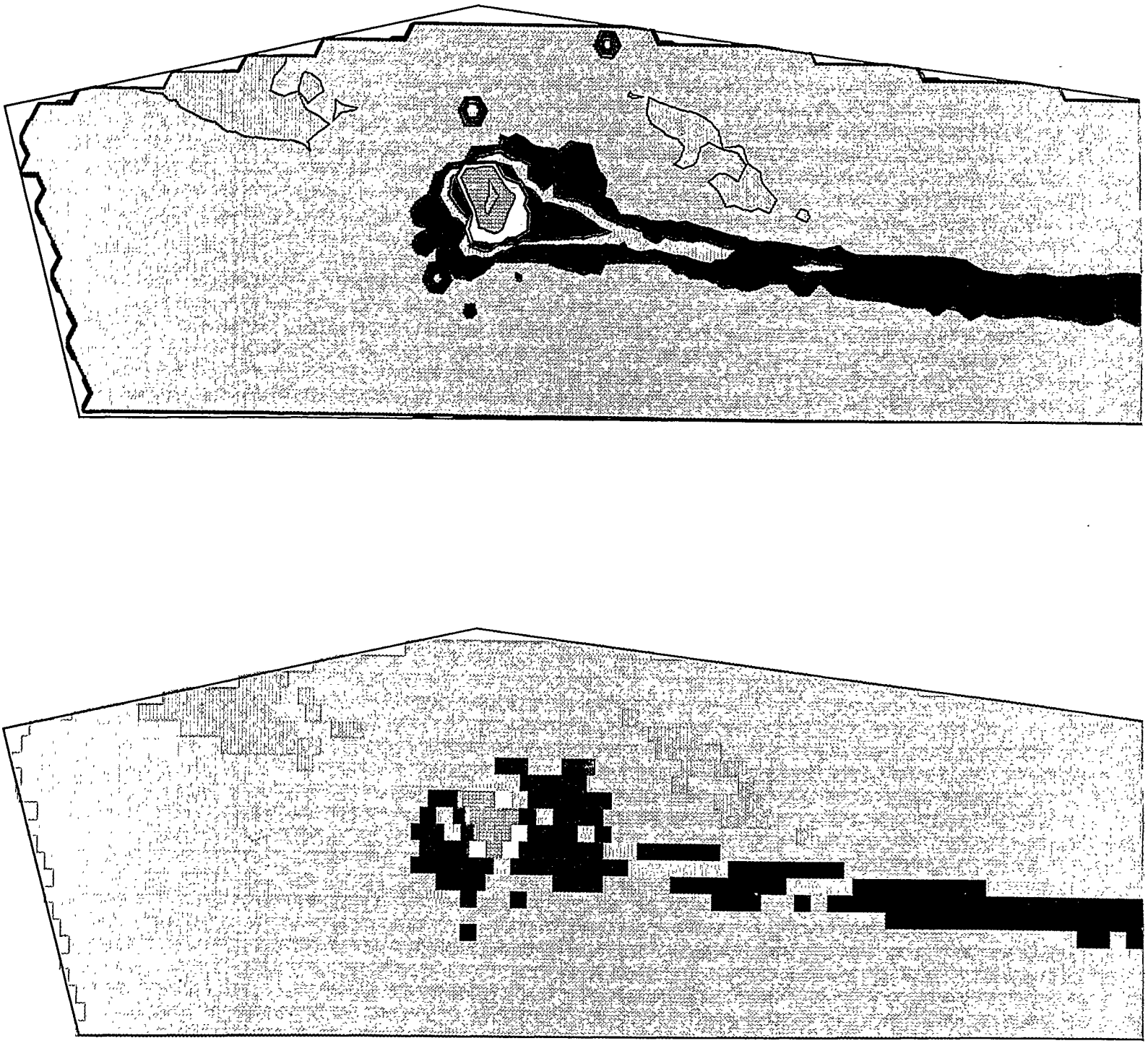

FIGURE 11. ***KIWI 30-FT GRIDDED AND 30-FT AVERAGED GROSS COUNT DATA.*** *The observed gross count of all gamma rays in the individual Kiwi spectra were collected into a 30-ft grid and averaged over one grid cell. Since the survey area is relatively small, the gross count rate is relatively constant, except in the heavily contaminated areas. The data are presented both as squares centered on the grid loci and as contour levels derived from the gridded data.*

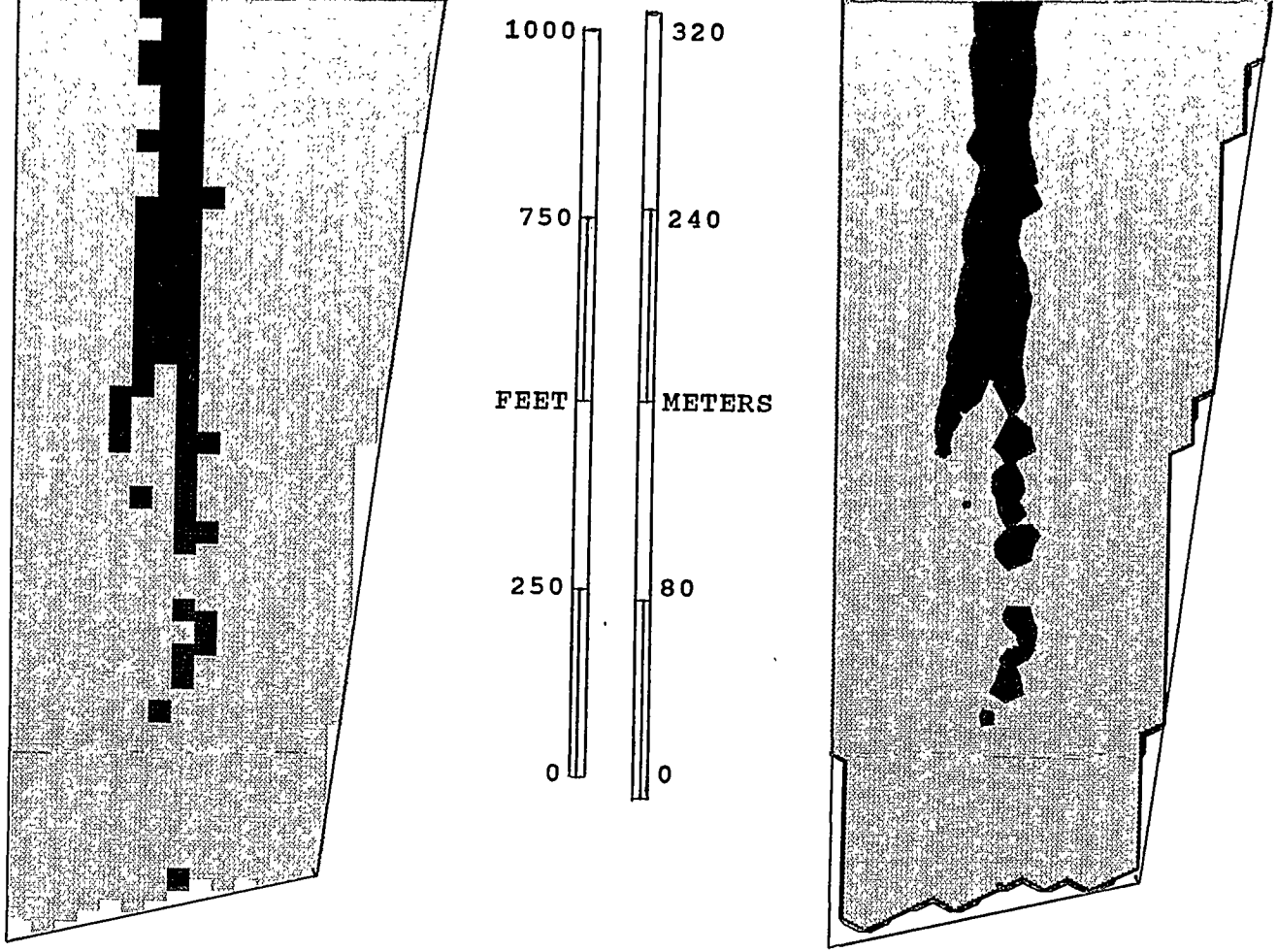

OBSERVED GROSS COUNTS PER SECOND
(40 keV THROUGH 3026 keV, 30′ GRID, 30′ AVG)

		GRAY	<	18000
18000	<	LT BLUE	<	19000
19000	<		<	20000
20000	<	LT GRN	<	21000
21000	<	GREEN	<	24000
24000	<	YELLOW	<	33000
33000	<	ORANGE	<	60000
60000	<	PINK	<	140000

NAFR DOUBLE TRACKS "KIWI" DATA - JUNE 1995

MAP PRODUCED 10/6/95 EG&G/EM

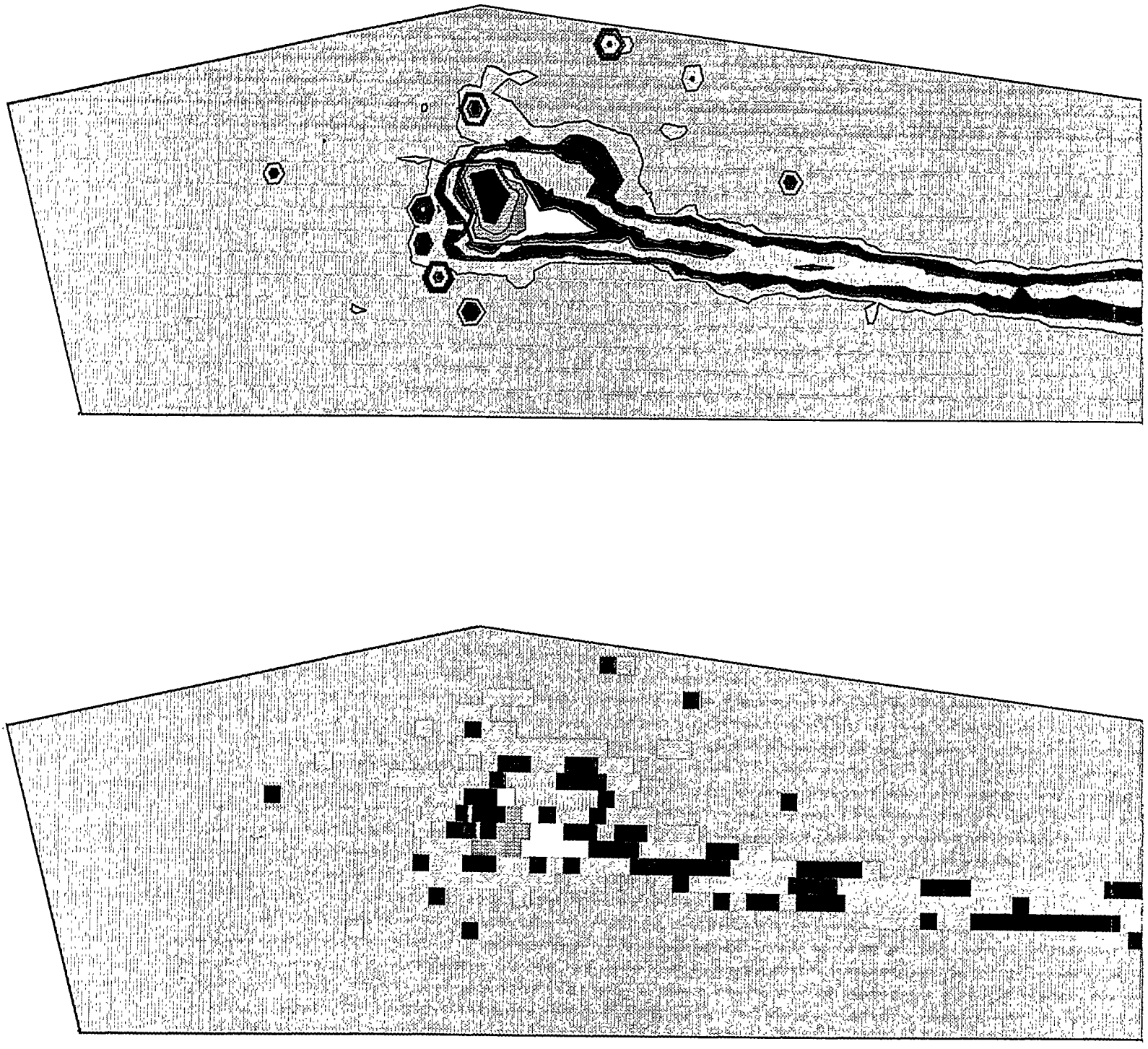

FIGURE 12. ***KIWI 30-FT GRIDDED AND 30-FT AVERAGED TRU ACTIVITIES.*** *These plots are based on the same data presented in Figure 10 except that the ^{241}Am counts have been collected into 30-ft averages and centered on a 30-ft grid. The data are presented both as squares centered on the grid loci and as contour levels derived from the gridded data.*

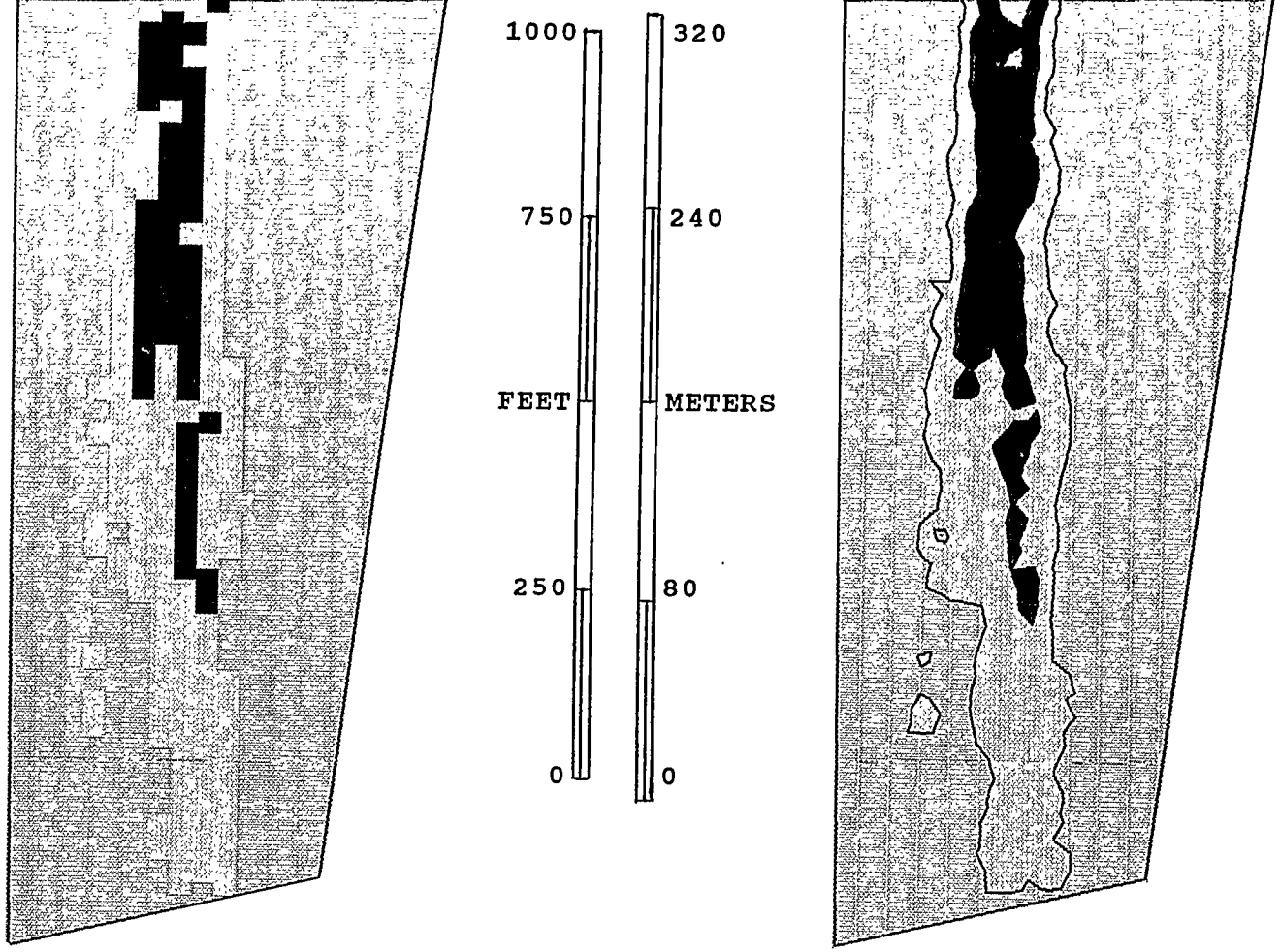

TOTAL TRANSURANIC PICOCURIES/GRAM
(FROM 3 WINDOW AM-241, 30′ GRID, 30′ AVG)

	GRAY	< 50		
50 <	LT BLUE	< 100	(189000 FT^2)	
100 <		< 200	(91800 FT^2)	
200 <	LT GRN	< 400	(56700 FT^2)	
400 <	GREEN	< 800	(20700 FT^2)	
800 <	YELLOW	< 1600	(7200 FT^2)	
1600 <	ORANGE	< 3200	(2700 FT^2)	
3200 <	PINK	< 6400	(2700 FT^2)	
6400 <		< 12800	(4500 FT^2)	

NAFR DOUBLE TRACKS "KIWI" DATA - JUNE 1995

MAP PRODUCED 10/6/95 EG&G/EM

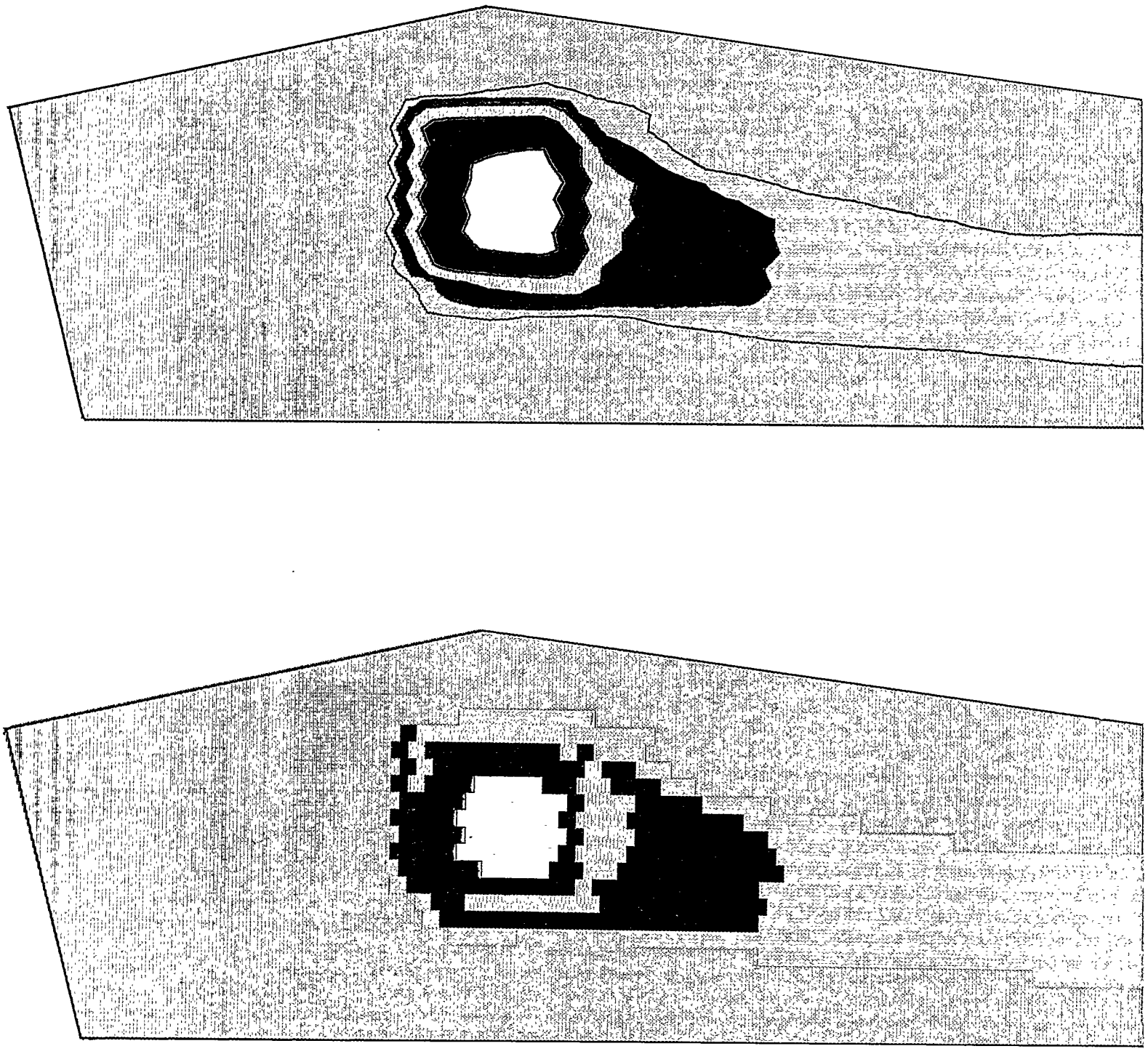

FIGURE 13. ***KIWI 30-FT GRIDDED AND 270-FT AVERAGED TRU ACTIVITIES.*** *These are the same data as in Figure 12, except that the ^{241}Am counts have been collected into 270-ft averages centered on a 30-ft grid. The 270-ft averages approximate the spatial resolution of the aerial system at 100 ft AGL. The data are presented both as squares centered on the grid loci and as contour levels derived from the gridded data. Note how well the contour levels in the GZ area match those of Figure 2 in reference 6 (or the aerial data presented as part of Figure 5 in this document).*

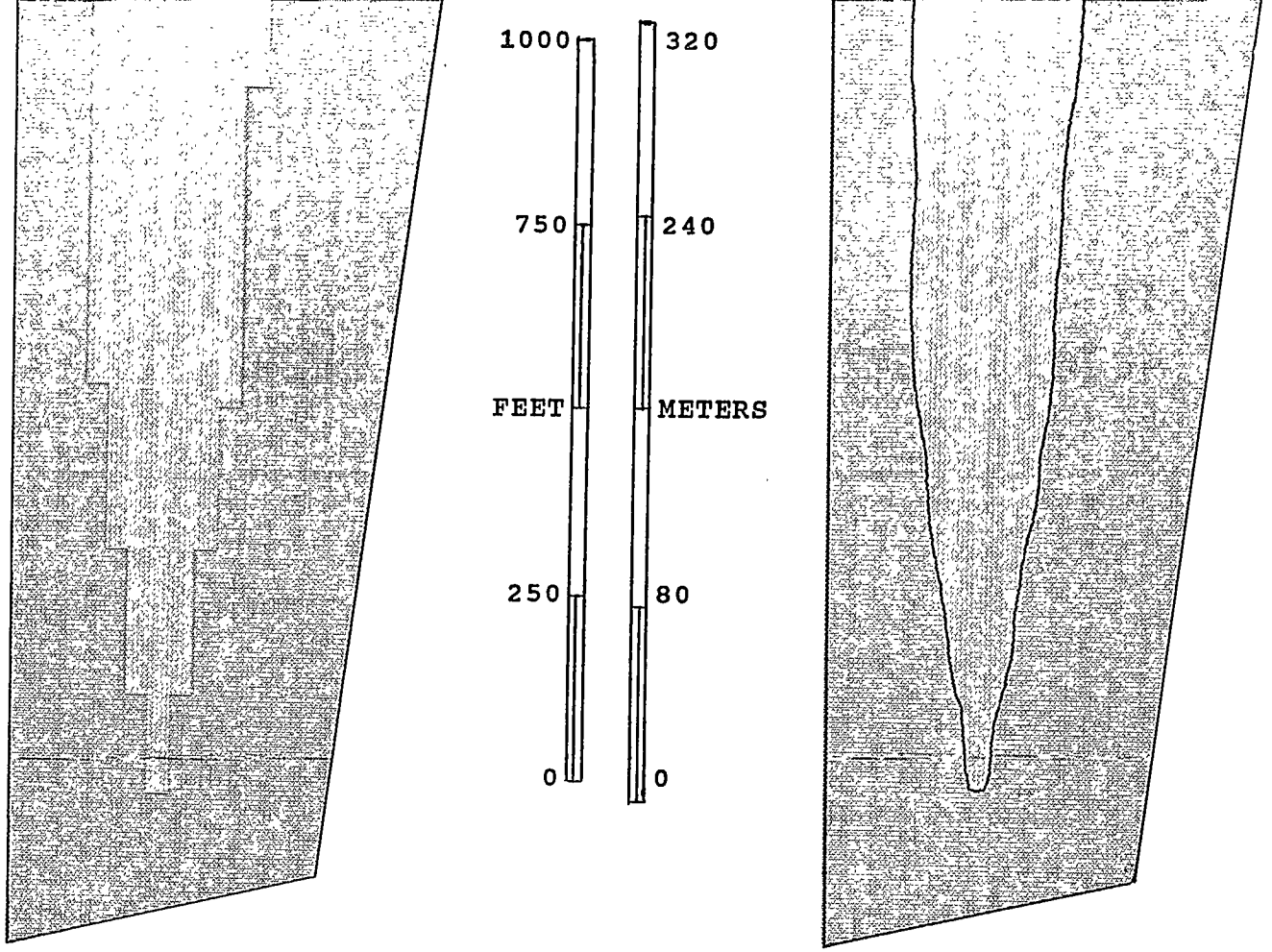

TOTAL TRANSURANIC PICOCURIES/GRAM
(FROM 3 WINDOW AM-241, 30′ GRID, 270′ AVG)

		GRAY	<	50
50	<	LT BLUE	<	100
100	<		<	200
200	<	LT GRN	<	400
400	<	GREEN	<	800
800	<	YELLOW	<	1600

NAFR DOUBLE TRACKS "KIWI" DATA - JUNE 1995

MAP PRODUCED 10/6/95 EG&G/EM

east side. Actually, this maximum contour should be much larger and encompass most if not all of the mound, but the linear interpolation distorts the values in this area. On the plots, the fence is reconstructed from the measured GPS positions of the corner positions. The jagged boundary of the data is a consequence of collecting data only inside the fence. The data are presented both as colored squares corresponding to the level of activity at each grid location and as contour levels enclosing regions of the same or higher activity.

The preparation of the data in Figure 12 is similar to that of the previous figure, except that this plot is based on the count rate in the photopeak of the 60-keV gamma rays from ^{241}Am. The TRU activity shown in the figure uses the 16:1 TRU:^{241}Am ratio calculated earlier. Here there is a much better definition of the plume area as well as more details of hot spots within a few hundred feet of the GZ area. As discussed earlier, the Kiwi did not travel over the mound, and those grid cells were filled with a linear interpolation of the data measured around the base of the mound. Therefore, no specific conclusions should be drawn about the ^{241}Am or TRU activity from the Kiwi data on top of the mound. For these data, all grid points outside the fenced area were given ^{241}Am activities of zero. Even with this assumption, it is clear the plume extends all the way to and through the southern fence (see results of the Suburban measurements in Section 6.6).

If a second averaging scale of approximately 90 m (270 ft) is used, the size of the grid footprint approaches the size of the aerial detector system footprint. Figure 13 shows the Kiwi TRU activity data using this new footprint. Notice the similarities in the contour shapes from the Kiwi data compared to the contour shapes from the aerial data in Figure 9 (recall that Figure 9 still uses the old TRU:^{241}Am ratio of 10:1). There is quite good agreement around GZ.

The Kiwi contours do not spread all the way to the eastern and western fences in the same way as the aerial data. This can be understood as a consequence of the aerial system not having a well-defined footprint. The Kiwi has Cd shielding on the sides of its detectors to limit detector visibility to the side. The aerial system has no shielding and the footprint is "defined" by the attenuation of the gamma rays traveling through the air to the detector. Thus a relatively weak source which is beyond the aerial system footprint can be ignored. However, a strong source (the mound) can contribute a few percent of its gamma rays to the aerial system even when it is well beyond the normal footprint limit, and therefore, it will produce an effect at large distances.

The agreement between the Kiwi and the aerial system is not quite as remarkable in the plume area. This may just be a result of the much lower activity and the aerial system's inability to do much with measurements made at or near its minimum detectable activity limit.

6.6 Experiment #6 (June)—HPGe *In Situ* Measurements

In June, the Suburban HPGe detector system made a series of measurements to establish background levels around the outside of the fence at Double Tracks and at the revegetation site northeast of Double Tracks. The locations and activity levels measured by the Suburban system are listed in Table 6. Figure 14 (see page 33) shows the locations marked by colored dots corresponding to the TRU activity. Again, the aerial and ground-based data in this figure both use a 16:1 ratio to convert the measured ^{241}Am activity to TRU activity.

As a check on the consistency of the data, the activity of a control point was measured at the beginning and end of each day. The results of these measurements are listed in Table 7 (see page 34). Once the Suburban went inside the exclusion zone, it stayed there until the end of the week. Thus two separate control points were established: one outside, which was used on the first day, and one inside, which was used on the remaining days. The two dots in Figure 14 identify the two control points. The ^{241}Am activity at the control points is very low (below the minimum detectable activity) and counting statistics dominate. The daily comparisons were made using the ^{40}K photopeak at 1,461 keV and the ^{228}Ac pair of photopeaks around 965 keV, which had sufficient counts in the 600-second measurements.

These control points also provided a check on the variations in the GPS positioning system. One second of latitude is approximately 31 m (101 ft) while one second of longitude is only about 24 m (80 ft). While the Suburban was returned daily to what visually appeared to be the same location, the variation appears to follow the 3-5 m (10-15 ft) accuracy of this particular GPS system.

Table 6. Suburban Measurements in June. The locations and Am concentrations are shown for the HPGe measurements made at the Double Tracks area. Excluded from the table are the energy calibration measurements. The TRU concentration is based on a (^{239}Pu + ^{240}Pu + ^{241}Am):^{241}Am ratio of 16. Positions shown in *italics* never received a lock on the differential GPS signal, so they have a positional uncertainty on the order of 100 m (300 ft).

File No.	Latitude (N)	Longitude (W)	^{241}Am (pCi/g)	TRU (pCi/g)
3	37°42′14.27″	116°59′14.87″	< MDA[a]	< MDA[a]
4	37°41′58.25″	116°59′18.54″	< MDA[a]	< MDA[a]
5	37°41′57.61″	116°59′23.62″	< MDA[a]	< MDA[a]
6	37°42′17.50″	116°59′22.65″	< MDA[a]	< MDA[a]
7	37°42′29.20″	116°59′21.83″	< MDA[a]	< MDA[a]
8	37°42′30.59″	116°59′14.97″	< MDA[a]	< MDA[a]
9	37°42′34.29″	116°59′ 0.66″	< MDA[a]	< MDA[a]
10	37°41′57.89″	116°59′21.10″	9.37 ± 0.58	149.9 ± 9.3
11	37°41′53.04″	116°59′21.30″	5.69 ± 0.56	91.0 ± 9.0
13	37°41′58.12″	116°59′21.44″	7.49 ± 0.56	119.8 ± 9.0
14	37°42′ 1.19″	116°59′21.74″	6.05 ± 0.55	96.8 ± 8.8
15	37°42′ 4.28″	116°59′21.13″	9.70 ± 0.59	155.2 ± 9.4
16	37°42′ 7.09″	116°59′20.11″	14.10 ± 0.62	225.6 ± 9.9
23	37°42′ 7.24″	116°59′20.38″	19.19 ± 0.66	307.0 ± 10.6
24	37°42′10.09″	116°59′20.00″	30.70 ± 0.73	491.2 ± 11.7
25	37°42′13.15″	116°59′20.14″	17.32 ± 0.65	277.1 ± 10.4
26	37°42′14.84″	116°59′19.75″	22.22 ± 0.70	355.5 ± 11.2
27	37°42′17.09″	116°59′19.38″	15.63 ± 0.65	250.1 ± 10.4
28	37°42′18.12″	116°59′19.41″	6.70 ± 0.57	107.2 ± 9.1
29	37°42′19.16″	116°59′19.14″	11.57 ± 0.62	185.1 ± 9.9
30	37°42′19.40″	116°59′18.82″	19.54 ± 0.67	312.6 ± 10.7
31	37°42′19.92″	116°59′18.73″	28.34 ± 0.74	453.4 ± 11.8
32	37°42′20.42″	116°59′18.47″	52.36 ± 0.90	837.8 ± 14.4
33	37°42′20.90″	116°59′18.24″	86.12 ± 1.06	1,377.9 ± 17.0
34	37°42′23.04″	116°59′17.45″	13.69 ± 0.63	219.0 ± 10.1
35	37°42′23.78″	116°59′17.21″	3.02 ± 0.52	48.3 ± 9.3
43	37°42′24.89″	116°59′16.72″	2.77 ± 0.53	44.3 ± 8.5
44	37°42′26.53″	116°59′16.09″	< MDA[a]	< MDA[a]
45	37°42′29.33″	116°59′15.10″	< MDA[a]	< MDA[a]
46	37°42′22.82″	116°59′22.16″	1.75 ± 0.51	28.0 ± 8.2
47	37°42′22.74″	116°59′20.81″	2.15 ± 0.53	34.4 ± 8.5
48	37°42′22.50″	116°59′19.50″	2.46 ± 0.53	39.4 ± 8.5
49	37°42′22.28″	116°59′18.98″	7.38 ± 0.58	118.1 ± 9.3
50	37°42′21.59″	116°59′16.55″	75.50 ± 1.04	1,208.0 ± 16.6
51	37°42′21.42″	116°59′16.17″	11.72 ± 0.61	187.5 ± 9.8

[a] The Minimum Detectable Activity (MDA) is equal to 3σ where σ is the standard deviation of the counting statistics. For measurements made at a height of 3 m, the MDA is 1.0 pCi/g of ^{241}Am and 16.0 pCi/g of TRU. For measurements made at a height of 7.5 m, the MDA is 1.5 pCi/g of ^{241}Am and 24.0 pCi/g of TRU.

Table 6. Suburban Measurements in June (continued)

File No.	Latitude (N)	Longitude (W)	^{241}Am (pCi/g)		TRU (pCi/g)	
52	37°42′21.19″	116°59′15.42″	6.15	± 0.57	98.4	± 9.1
53	37°42′21.24″	116°59′14.92″	7.57	± 0.57	121.1	± 9.1
54	37°42′20.91″	116°59′14.25″	4.58	± 0.53	73.3	± 8.5
55	37°42′20.72″	116°59′13.51″	< MDA[a]		< MDA[a]	
56	*37°42′21.10″*	*116°59′17.20″*	19.43	± 0.67	310.9	± 10.7
57	37°42′20.34″	116°59′17.35″	46.25	± 0.85	740.0	± 13.6
58	*37°42′20.60″*	*116°59′19.00″*	2.57	± 0.55	41.1	± 8.8
59	37°42′21.63″	116°59′19.69″	1.86	± 0.52	29.8	± 8.3
60	37°42′20.61″	116°59′19.58″	< MDA[a]		< MDA[a]	
61	37°42′19.82″	116°59′17.24″	17.50	± 0.66	280.0	± 10.6
73	37°42′20.04″	116°59′15.51″	4.76	± 0.55	76.2	± 8.8
74	37°42′18.02″	116°59′16.84″	3.54	± 0.55	56.6	± 8.8
75	37°42′16.67″	116°59′16.24″	1.78	± 0.51	28.5	± 8.2

[a]The Minimum Detectable Activity (MDA) is equal to 3σ where σ is the standard deviation of the counting statistics. For measurements made at a height of 3 m, the MDA is 1.0 pCi/g of ^{241}Am and 16.0 pCi/g of TRU. For measurements made at a height of 7.5 m, the MDA is 1.5 pCi/g of ^{241}Am and 24.0 pCi/g of TRU.

6.7 Experiment #7 (June)—Hot-Piece Activity Measurements

Results of the metallic piece measurements are given in Table 8 (see page 35). Most pieces were relatively flat and approximately 0.5 to 1.0 cm (0.2-0.4 in) thick. Assuming that the pieces were thick enough to stop the ^{241}Am 60-keV gamma ray, the total activity contained on a piece is the sum of that obtained from measuring each side. By dividing this total by the mass of the piece, the activity per unit mass can be determined. These results, for both ^{241}Am and TRU, are also presented in Table 8. As shown in this table, all these pieces greatly exceed the level (0.1 μCi/g) currently used to separate TRU waste from low-level waste.

Table 9 (see page 36) presents the results of the soil sample measurements. The lower density of the soil (compared to the metallic pieces discussed above) and the size of the bottles allow some fraction of the ^{241}Am 60-keV gamma rays to escape through either side of the bottle. Thus a measurement of both sides may count the activity of a location in the bottle twice. The TRU values given in the table are based on the sum of the activity measured from each side. The actual total soil activity should be somewhere between the value obtained from one side and the sum of the activity measured from both sides. The data show that some very small areas within the inner fence have activity levels slightly greater than that used to define TRU waste. However, the areas involved are quite small compared to the total area that will have soil removed during the remediation. Most of the soil to be removed has activity levels well below the TRU level. Therefore, the bulk soil transported off-site for disposal should fall well within the classification used for low-level waste.

7.0 SUMMARY

A series of measurements were conducted at the Double Tracks site on Stonewall Flat at the NAFR. The April expedition tested a number of new techniques and performed several preliminary characterization measurements. In addition, three techniques for rapidly assessing the Am and Pu depth profiles were tested. Several plots comparing these ground-based system measurements with each other and with the 1993 aerial data show remarkable agreement.

The June expedition focused on the site characterization using the newly designed Kiwi vehicle. Another new detector platform, an ATV equipped with FIDLER detectors, performed a search for hot pieces marking the locations for later removal by teams of "miners."

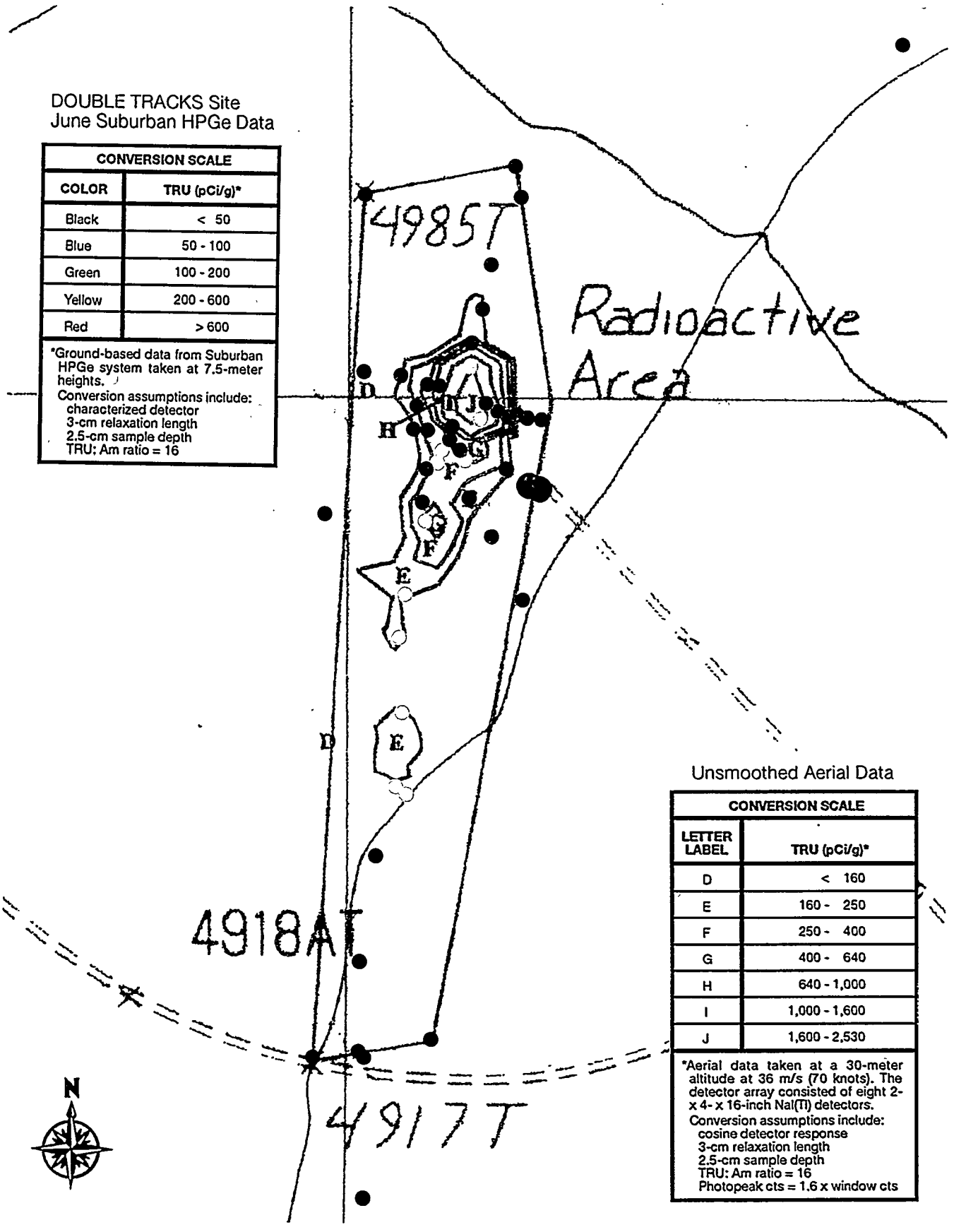

FIGURE 14. *MEASUREMENT LOCATIONS OF THE SUBURBAN SYSTEM (JUNE). The locations (by GPS coordinates) of the Suburban measurements are marked by colored dots corresponding to five bands of TRU activity. The contour data from the 1993 aerial survey are included for reference. Both sets of data use the 16:1 TRU:^{241}Am activity ratio. The two control points (one inside the fence and one outside) are indicated by the large dots.*

Both of these new systems performed better than expected.

For future site characterizations, the ATV will search for hot pieces. The tripod HPGe systems will obtain rough depth distributions in the soil and measure isotopic ratios. The Suburban system with the HPGe detector suspended on the end of a mast will make spot measurements inside the contaminated area as well as a set of measurements to establish background radiation levels. Once all of this work is complete and these systems leave the area, the Kiwi system will perform the actual characterization measurements of the site. The Kiwi will use the depth distributions and isotopic ratios to calculate accurate soil concentration and the horizontal distribution of the contamination.

Table 7. Control Point Suburban Measurements in June. The locations and isotopic concentrations are shown for the HPGe measurements made at the daily control points. Positions shown in *italics* never received a lock on the differential GPS signal, so they have a positional uncertainty on the order of 100 m (300 ft).

File No.	Latitude (N)	Longitude (W)	^{228}Ac (pCi/g)		^{40}K (pCi/g)	
Outside Fence						
2	37°42′18.55″	116°59′13.48″	not recorded			
12	37°42′18.44″	116°59′13.54″	3.38	± 0.24	63.5	± 1.3
Inside Fence						
22	37°42′19.25″	116°59′14.00″	not recorded			
36	37°42′18.91″	116°59′14.25″	2.92	± 0.22	57.2	± 1.3
42	*37°42′20.34″*	*116°59′14.99″*	3.15	± 0.23	60.5	± 1.3
62	37°42′18.94″	116°59′14.06″	2.71	± 0.24	57.6	± 1.3
72	37°42′18.70″	116°59′14.06″	3.33	± 0.23	58.8	± 1.2
76	37°42′18.67″	116°59′14.15″	3.00	± 0.23	57.7	± 1.3

Table 8. "Pieces" Activity Measurements from June. Selected pieces of metal, coated with an Am and Pu mixture, were collected and measured during the June survey. Their specific activity measurements place them in the TRU waste category. Note that the activities in this table are μCi/g rather than the pCi/g used throughout the rest of the report.

Piece Number	^{241}Am Activity Side 1 (μCi)	^{241}Am Activity Side 2 (μCi)	^{241}Am Activity Total (μCi)	Mass (g)	^{241}Am Act./mass (μCi/g)	TRU[a] Act./mass (μCi/g)
06/07/95[b]						
1	143.7	179.5	323.2	33.25	9.7	155
2	71.4	89.0	160.4	30.68	5.2	84
3	357.1	255.5	612.6	254.01	2.4	39
4	318.3	366.1	684.4	316.4	2.2	35
5	167.0	144.5	311.5	124.12	2.5	40
6	157.8	211.3	369.1	58.87	6.3	100
7	54.2	54.2	108.4	13.41	8.1	130
10	106.2	120.4	226.6	95.55	2.4	38
11	17.7	17.6	35.3	21.33	1.7	27
12	49.6	54.8	104.4	2.4	43.5	696
06/08/95[c]						
13	87.7	74.3	162.0	107.36	1.5	24
14	123.3	123.3	246.6	39.78	6.2	99
15	38.5	47.7	86.2	17.38	5.0	80

[a] Assumed a TRU to ^{241}Am ratio of 16. Note: TRU waste is defined as an activity/mass greater than 0.1 μCi/g.
[b] Subtracted a background activity of 5.4 μCi.
[c] Subtracted a background activity of 1.3 μCi.

Table 9. Soil Sample Activity Measurements from June. Selected soil samples measured during the June expedition exhibit Am and TRU activity levels higher than the definition of TRU waste. For soil sample counting, the actual value will probably be closer to that obtained from one side only, which would be approximately half the value quoted here. Note that the activities in this table are μCi/g rather than the pCi/g used throughout the rest of the report.

Sample Number	^{241}Am Activity Side 1 (μCi)	^{241}Am Activity Side 2 (μCi)	^{241}Am Activity Total (μCi)	Mass (g)	^{241}Am Act./mass (μCi/g)	TRU[a] Act./mass (μCi/g)
06/07/95[b]						
8	2.5	3.8	6.3	796.62	0.008	0.128
9	8.2	6.0	14.2	746.97	0.019	0.304
06/08/95[c]						
S1[d]	2.3	2.4	4.7	558.41	0.008	0.134
S2[e]	5.9	6.3	12.2	240.87	0.051	0.816
S3[f]	4.6	5.0	9.6	297.77	0.032	0.512
S4[g]	5.8	5.7	11.5	345.86	0.033	0.528

[a] Assumed a TRU to ^{241}Am ratio of 16. Note: TRU waste is defined as an activity/mass greater than 0.1 μCi/g.

[b] Subtracted a background activity of 5.4 μCi. Samples were taken from soil previously collected from areas within the exclusion area which were identified by the FIDLER detectors on the ATV as containing elevated amounts of Am.

[c] Subtracted a background activity of 1.3 μCi.

[d] Sample was collected approximately 20 m (60 ft) from GZ in direction of 65°.

[e] Sample taken approximately 1.6 m (5 ft) below ground level during the drilling operations to assess the contents of the mound at GZ.

[f] Sample taken approximately 30 m (100 ft) east of GZ.

[g] Sample taken approximately 45 m (150 ft) east of GZ.

APPENDIX A

SURVEY PARAMETERS AND RESULTS

Parameters

Survey Site:	Double Tracks Site Nellis Air Force Range near Tonopah, Nevada
Survey Dates:	April 10-13, 1995 June 5-9, 1995
Nominal Site Elevation:	1,450-1,550 m (4,800-5,000 ft) MSL
Survey Altitude:	0.75 m (30 in) Kiwi (NaI) system 0.75 m (30 in) ATV (FIDLER) system 1 m (3 ft) HPGe tripods 3 m (10 ft) and 7.5 m (25 ft) Suburban (HPGe) system
Line Spacing:	3 m (10 ft) Kiwi system 1.6 m (5 ft) ATV system
Line Direction:	Kiwi: north-south inside fenced area and approximately northwest-southeast south of fenced area. ATV: east-west inside fence.
Survey Coverage:	Approximately 0.13 km^2 (0.05 mi^2) inside fenced area. Sporadic measurements outside fenced area.
Base of Operation:	Tonopah Test Range, Nevada.
Positioning System:	Differential GPS (Global Positioning System).
Detector Arrays:	Two tripod systems: approximately 86% and 107% efficiency HPGe. Suburban vehicle with approximately 98% HPGe on extendable mast. Kiwi vehicle with NaI detectors and REDAR IV. ATV with three FIDLER detectors.

Conversion Factors

1 μR/h = 8.76 mR/yr ≈ 8.37 mrem/yr

APPENDIX B

This appendix is an unpublished internal report of some work performed in Area 11 of the NTS and is included here principally for its background information on the thermoluminescent detector (TLD) sheets and to highlight the discrete distribution of Pu at another site. One of the authors of this appendix (AB) assisted in the data collection at Double Tracks. Minor editorial changes have been made to the original document.

IN SITU MEASUREMENT OF ENVIRONMENTAL ALPHA ACTIVITY AT VERY HIGH SPATIAL RESOLUTION AND SENSITIVITY

A. BHATTACHARJIE AND W. QUAM
EG&G/EM SANTA BARBARA OPERATIONS

Abstract

Large (30 cm by 30 cm) TLD sheets were used to determine the surface and depth distribution of ^{239}Pu alpha contamination at a location on the Nevada Test Site. The spatial resolution was 3 mm at a signal to noise ratio exceeding 20 to 1. Depth profiles were analyzed to derive their characteristic shape. Selected graphs of the raw alpha distributions, from surface and depth distributed activities, are shown.

Introduction

Recent work by International Sensor Technology (IST) in Pullman, WA, has yielded several large area TLD products. One such TLD, a calcium sulfate (thulium activator) was used for the *in situ* alpha contamination measurements reported here. These TLD materials are provided in sheet form approximately 30 cm by 30 cm with individual TLD's located on 3-mm centers on the surface of the Kapton backing. The TLD material is held on the sheet surface with a binder of a few microns thickness. The alpha sensitivity is sufficient to activate the TLD traps in the TLD material.

The TLD sheets are robust and may be readily handled for placement. The sheets are reusable and can be readout several hundred times. The TLD sheets are sensitive to betas and gammas as well as alphas; however, the higher linear energy transfer of the alpha produces a larger signal per incident particle. Thus the sheets can be used to discriminate between the three radiations by setting up a discrimination threshold based upon signal to noise ratio.

Calibration measurements with ^{241}Am show that the sensitivity of this TLD material was 0.3 pCi for a 20-minute exposure time. We believe that this sensitivity can be increased by a large margin by improving the readout technique. The manufacturer (Dr. Braunlich of IST) has stated that recent improvements in readout technique can yield up to a factor of 100 in alpha detection sensitivity.

Description of the Field Experiment

The measurements were performed on several occasions within the fenced Site B in Area 11 at the Nevada Test Site. This area is available for evaluation of detectors that are not usually used for *in situ* measurements. The present work was performed for a DOE environmental restoration project.

The TLD sheets were manually placed on the soil surface to create surface maps and pressed vertically into the subsurface with a hammer-driven emplacement tool to create vertical profile maps. The major objectives were to observe the detector performance in high ground temperatures with sun at zenith and to determine feasibility of locating minute plutonium "hot particles" on site. Exposure times of 15 to 70 minutes were used, with good data

obtained over this range. After exposure the TLD's were read out with an IST automatic reader using a pulsed carbon dioxide laser. The readout process takes about one hour.

The data are obtained as a three-dimensional array and can be drawn as an XYZ plot from a personal computer file with the alpha activity plotted as the Z coordinate and the soil surface shown as the XY plane. These files can readily be manipulated to determine the statistical parameters of alpha activity within user-selected XY domains.

Three different TLD sheet materials were field tested to determine noise figures and detection sensitivities. Although ground temperatures were not measured, the air temperature was in the vicinity of 108° F; *i.e.*, less than ideal for this material. Nonetheless, the data obtained were fairly noise free, with calcium sulfate (thulium activator) being the most sensitive. The figures shown are from this material.

Discussions

As mentioned earlier, the measurements were performed at Site B in Area 11 at the Nevada Test Site. This area was used many years ago for safety shots and has a surface contamination of ^{239}Pu. Cleanup of this area is currently in process.

The first plot shows the XYZ representation of data from one TLD sheet laid flat on the soil surface and exposed for 30 minutes with part of its sensitive surface covered with an alpha absorber. This measurement served to prove that the isolated large peaks were caused only by alpha. They are present in the uncovered part and not (with some exceptions) in the covered part. The peaks seen in the covered part are noise peaks caused by readout errors and would cause false alarms. The background outside the large spikes is a combination of real incident background and the noise generated during readout. These plots show nearly 10,000 pixels of data points, each the reading of an individual TLD.

The second plot is a representation of subsurface alpha activity. The TLD sheet was emplaced in the form of a cylinder about 6 cm in diameter. It was allowed to overlap and to extend above the soil surface. The plot shows a greatly reduced signal in the overlap region, again demonstrating that the origin of the spikes is incident alpha. Further, as expected, it shows a reduced signal in the above ground portion illustrating the higher alpha rate from soil. The third plot has been calculated from the subsurface data by integrating signal along the sheet's circumference and plotting versus depth. We see here that the alpha contamination is not uniform with depth but appears to be low for a few centimeters and then a sharp increase appears which gradually decreases versus depth. This behavior may be due to an uncontaminated overburden placed to minimize spread of the ^{239}Pu.

Conclusions

Our measurements have shown that the large area, high spatial resolution TLDs provide unique capabilities for environmental cleanup of plutonium and transuranics. Its *in situ* usage allows pinpointing contaminants without soil removal and processing. The disposal problem is simplified. Its large area allows large soil surface coverage in reasonable mapping times. With future improvements of TLD detection sensitivities, the mapping times would be significantly reduced. Further, the sheet TLDs provide a simple quantitative means of processing surface contamination with high spatial resolution. Minute "hot particles" would be located. Quantitative measurements of alpha contamination versus depth in soil may be readily obtained without taking soil samples for wet chemistry at a fraction of cost and time. Cost is additionally reduced by reusing the TLD sheets.

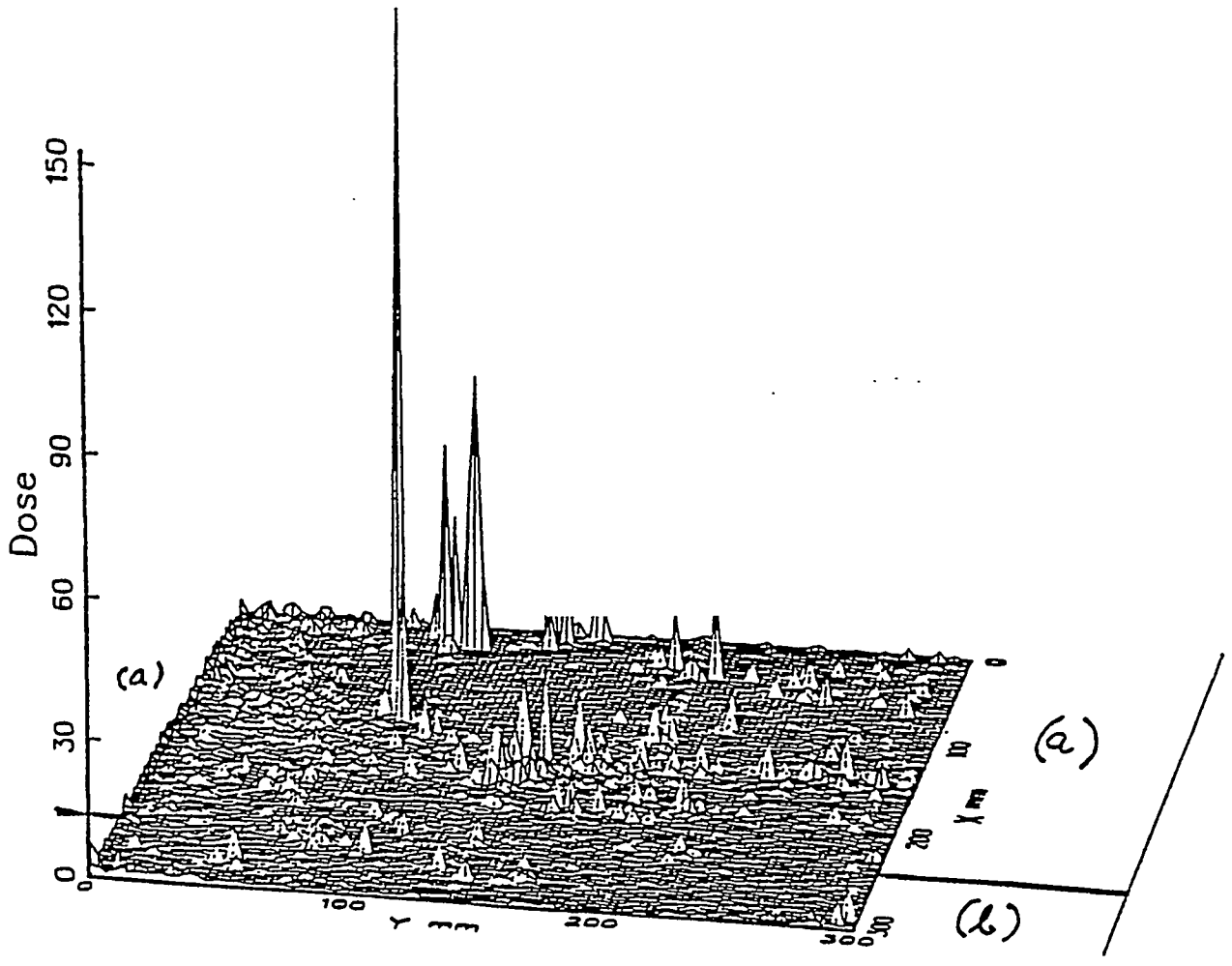

FIGURE B-1. *SOIL SURFACE ALPHA MAP WITH $CaSO_4$Tm (Grain Size 10 to 40 microns). Plot showing three-dimensional representation of 10,000 pixels of data points with the TLD sheet flat on the soil surface and exposed for 30 minutes (a) exposed section (b) section covered with an alpha absorber.*

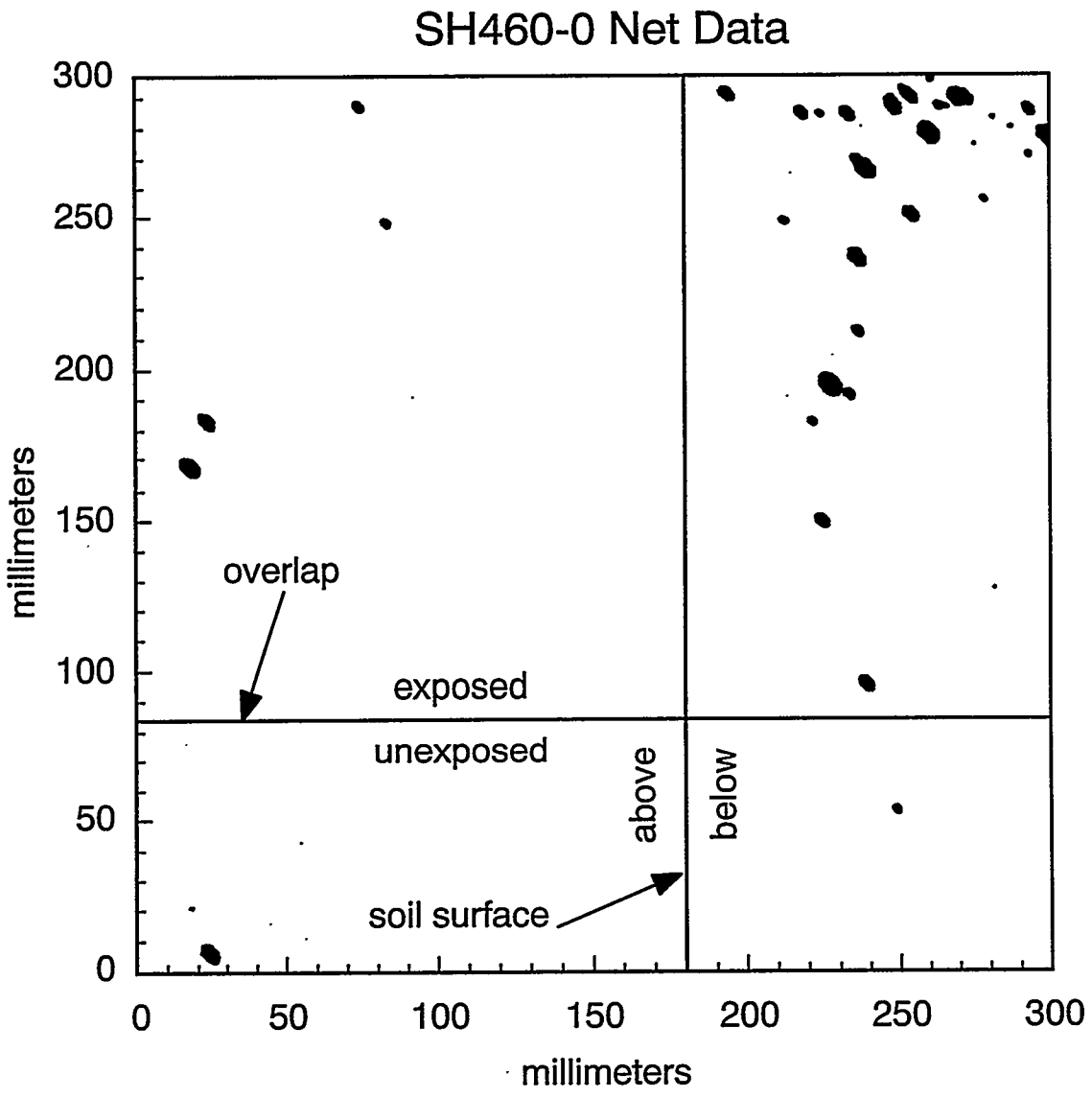

FIGURE B-2. ***PLOT OF SUBSURFACE ALPHA ACTIVITY. Dark spots are net signals covering several pixels each. The average background was 6,000 signal units and the largest peak was 400,000 signal units.***

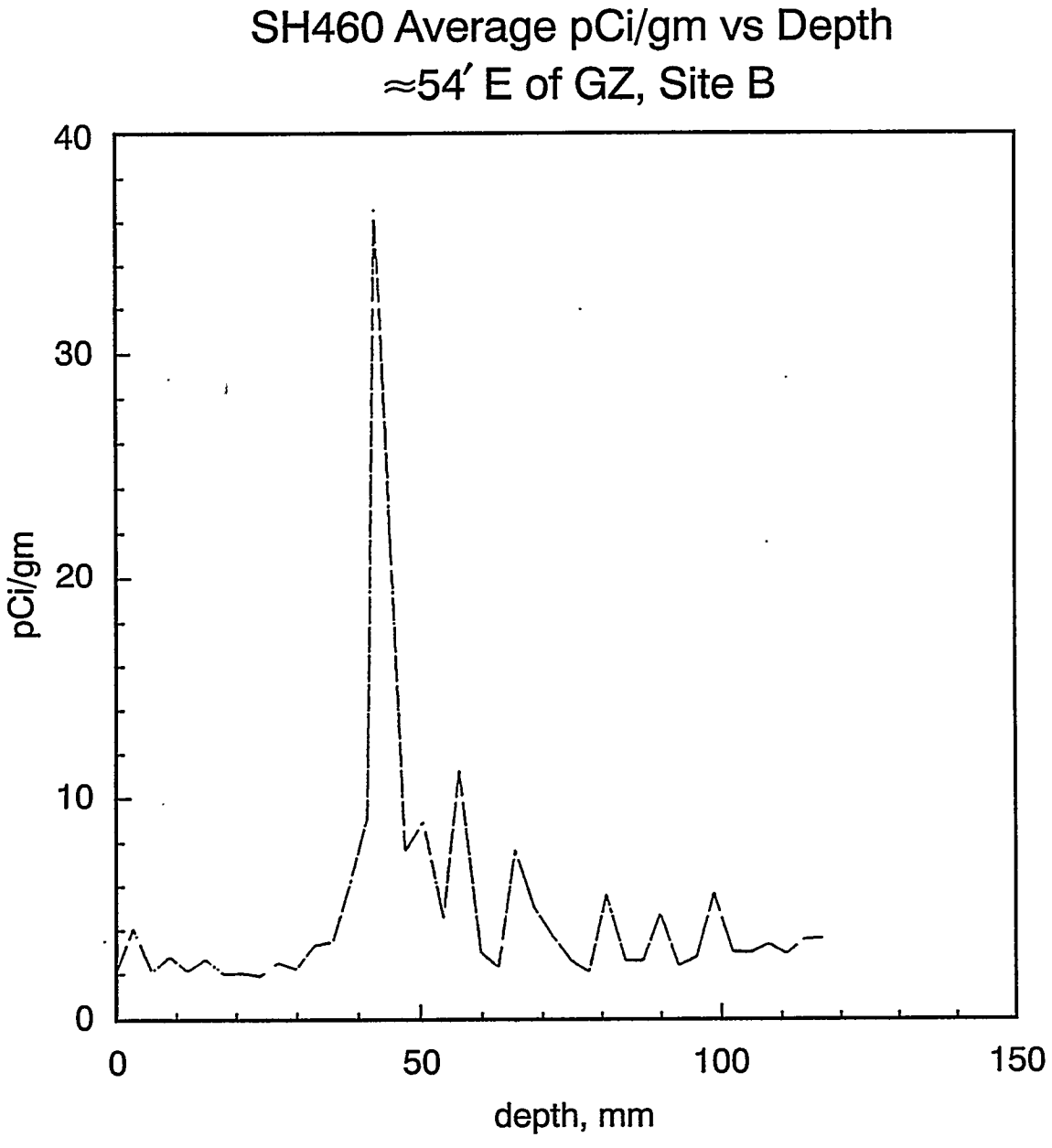

FIGURE B-3. ***THIS PLOT IS DERIVED FROM FIGURE B-2 AND REPRESENTS THE AVERAGE NET SIGNAL PER MINUTE INTEGRATED OVER THE TLD SHEET PORTION THAT WAS SUBSURFACE. Note that the signal to noise ratio is about 10:1 at 5 cm depth. The low signal between 0 and 5 cm may be due to clean soil overburden used to inhibit resuspension.***

REFERENCES

1. Schoengold, C.R., M.E. DeMarre, and E.M. McDowell. *Radiological Effluents Released from Announced U.S. Continental Tests 1961 Through 1988.* Report No. DOE/NV/317, REECo, Las Vegas, Nevada, 1990.

2. *Radiological Conditions at Project Roller Coaster Sites — 1966*, Report No. NVO-162-28. REECo, Mercury, Nevada, 1967.

3. Jobst, J.E. *An Aerial Radiological Survey of Clean Slates 1, 2, and 3, and Double Track*, Report No. EGG-1183-1737. EG&G, Las Vegas, Nevada, 1979.

4. Proctor, A.E., T.J. Hendricks. *An Aerial Radiological Survey of the Double Track Site and Surrounding Area*, Report No. EGG-11265-1086. EG&G/EM, Las Vegas, Nevada, 1994.

5. Hendricks, T.J. *Double Track Site*, Report No. EGG-11265-1146. EG&G/EM, Las Vegas, Nevada, 1995.

6. Lindeken, C.L., K.R. Peterson, D.E. Jones, and R.E. McMillen. "Geographical Variations in Environmental Radiation Background in the United States," *Proceedings of the Second International Symposium on the Natural Radiation Environment, August 7-11, 1972, Houston, Texas.* National Technical Information Service, Springfield, Virginia, pp 317-332, 1972.

7. Klement, Jr., A.W., C.R. Miller, R.P. Minx, and B. Shleien. *Estimates of Ionizing Radiation Doses in the United States 1960-2000*, U.S. EPA Report ORP/CSD72-1. EPA, Washington, D.C., 1972.

8. Reiman, R.T. *In Situ Surveys of the U.S. Department of Energy's Rocky Flats Plant — Golden, Colorado*, Report No. EGG-10617-1129. EG&G/EM, Las Vegas, Nevada, 1991.

9. Beck, H.L., J. DeCampo, and C. Gogolak. *In Situ Ge(Li) and NaI(Tl) Gamma Ray Spectrometry*, Report No. HASL-258, TID-4500. U.S. AEC Health and Safety, Laboratory, New York, New York, 1972.

DISTRIBUTION

DOE/DP

L. E. Gordon-Hagerty	(1)
O. W. Taylor	(1)

DOE/HQ

OSTI	(25)

DOE/NV

M. R. Dockter	(1)
M. Sanchez	(1)
Public Reading Room	(1)
TIO	(1)
TIRC	(1)

IT

J. R. McKinley	(3)

BN

P.P. Guss	WAMO	(1)
R.E. Kelley	LVAO	(1)
D.S. Long	LVAO	(1)
C. L. Lyons	LVAO	(1)
T E. Richardson	LVAO	(1)
S.R. Riedhauser	LVAO	(1)
W. J. Tipton	LVAO	(1)

LIBRARIES

RSL	(60)
WAMO	(1)

IN SITU RADIOLOGICAL SURVEYING AT
THE DOUBLE TRACKS SITE
NELLIS AIR FORCE RANGE
TONOPAH, NEVADA
DOE/NV/11718-013

DATE OF SURVEY: APRIL 10-13, 1995 AND JUNE 5-9, 1995
DATE OF REPORT: APRIL 1996